ADVANCED NANOBIOMED RESEARCH Open Access
www.advnanobiomedres.com

Multichannel Fluorescence Microscopy: Advantages of Going beyond a Single Emission

Paloma Rodríguez-Sevilla, Sebastian A. Thompson, and Daniel Jaque*

Fluorescent microscopy has enabled the study of intracellular processes and revealed the most intricate details of the subcellular structure. This has benefitted not only the basic biological science, but also has had an impact in numerous biomedical applications. Basic fluorescent sensing techniques use the change in the absolute emission of a fluorescent sensor. This entails some disadvantages as the signal might be influenced by factors not directly related to the process under study (e.g., fluctuations in the excitation source). To overcome these drawbacks, one can use multiple emissions of a single or various fluorophores. There are numerous examples of multichannel fluorescence microscopy techniques that have given rise to numerous ratiometric methods and multiplexing assays. Herein, how the use of multiple emission channels has impacted fluorescence microscopy in terms of speed, sensitivity, and resolution is reviewed. Using recent examples, how the easy implementation of multichannel detection can overcome current limitations of the main used fluorescence techniques and promote the development of novel microscopy methods is shown.

1. Introduction

Fluorescence microscopy has been proven to be an invaluable and versatile tool for medical diagnosis.[1] In the case of infectious diseases, pathogens such as bacteria, fungi, or viruses can be easily and specifically detected using targeted fluorescence labels, for example, antibodies that bind to a specific antigen in immunofluorescence tests.[2] Beyond this, fluorescence microscopy is widely used to study the onset and development of diseases and assess the action of medicaments.[3,4]

This is all based on the study of intracellular processes, molecules and organelles, and the bulk properties of the cells (e.g., viscosity, pH, temperature) which can be facilitated using fluorescent agents based on proteins, dyes, or particles.[5,6] Each of these fluorescent markers presents different advantages and disadvantages. For example, cells can be transfected with fluorescent proteins or reporter genes, so they can self-produce the fluorescent contrast agent. This reduces the toxicity introduced by exogenous agents, such as dyes and fluorescent particles. However, the transfection process is slow, sometimes not very efficient for certain types of cells, and it cannot currently be used in the clinic. Quick labeling (within minutes) can be achieved using fluorescent dyes. There is a wide library of commercial fluorescent dyes emitting along the whole visible spectra (reaching even the near-infrared) and that can target any region or organelle of the cell.[7,8] In addition, the staining procedure is usually simpler and faster than transfection or intracellular incorporation of particles: cells need hours to uptake particles via endocytosis or days to genetically express the fluorescent proteins, while the small size of the dye molecules, around 2 nm, and their hydrophobic nature allow them to faster enter the cell via diffusion.[9–11] On the other hand, fluorescent dyes, as well as luminescent particles, are known to induce some stress to live cells or present some unspecific intracellular staining.

Luminescent particles offer other advantages to fluorescent dyes such as better fluorescence stability (i.e., reduced photobleaching) and versatility. Currently, it is possible to find luminescent particles emitting from the UV to the infrared. In addition, they can be engineered to present special fluorescent characteristics such as persistent luminescence,[12,13] where the emission lasts long after the excitation is interrupted, or upconversion emission,[14,15] where the absorption of multiple low energy photons (e.g., infrared radiation) results in an emission

P. Rodríguez-Sevilla, D. Jaque
Nanomaterials for Bioimaging Group (NanoBIG)
Departamento de Física de Materiales
Universidad Autónoma de Madrid
C/Francisco Tomás y Valiente 7, Madrid 28049, Spain
E-mail: paloma.rodriguez@uam.es

S. A. Thompson
Madrid Institute for Advanced Studies in Nanoscience (IMDEA Nanociencia)
C/Faraday 9, Madrid 28049, Spain

S. A. Thompson
Nanobiotechnology Unit Associated to the National Center for Biotechnology (CNB-CSIC-IMDEA)
Madrid 28049, Spain

D. Jaque
Instituto Ramón y Cajal de Investigación Sanitaria
Hospital Ramón y Cajal
Ctra. Colmenar km. 9,100, Madrid 28034, Spain

The ORCID identification number(s) for the author(s) of this article can be found under https://doi.org/10.1002/anbr.202100084.

DOI: 10.1002/anbr.202100084

of higher energy (e.g., visible light). There is a large variety of luminescent particles that are used in microscopy studies, such as semiconductor nanocrystals,[16] metallic nanoparticles (NPs),[17,18] carbon-based nanomaterials,[19] rare-earth (RE)-doped particles,[20] and silica-based particles.[21,22] In addition, the development of synthetic methods makes it possible the combination between different emitting agents, including particles and organic-based molecules, for the construction of fluorescent nanocomposites with combined properties that can be used as fluorescent sensors at the nano- and microscale.[23,24]

Fluorescent sensing takes advantage of the effect of the surrounding medium on the emission properties of the fluorescent reporter (i.e., the probe or sensor).[25,26] The emission of fluorescent molecules and particles can be influenced by changes in the characteristics of the surrounding medium (e.g., temperature, pH, viscosity, or ion concentration), and this can be harnessed for sensing. Fluorescence-based sensing usually makes use of the intensity of a single emission that depends on, ideally, one characteristic/parameter of the surrounding medium. This entails some drawbacks and limitations, such as the dependence on the local concentration of the emitting probe, which reduces the reliability of the measurement. However, studies have proven the utility and enhanced sensing capability and reliability when using more than one emission.

As we discuss in this review, multiple channel techniques take advantage of the various emissions of a single or several emitters. The basic example is routine multilabeling, where the cells under study are stained with two or more fluorophores to simultaneously visualize different cellular regions or organelles (i.e., the nucleus and the cellular membrane) in different colors or channels. Also, more reliable sensing probes can be engineered using fluorophores with multiple emission bands. In addition, the utilization of multiple emissions offers new features that have an impact on the speed, complexity, sensitivity, and resolution of the measurement.[27]

This review is aimed to explain the benefits of using multiple emissions or color channels in fluorescence microscopy. We aim to make the readership working on a specific technique to easily understand how going beyond the use of the total intensity in a particular color channel can benefit their specific field of study. We provide examples of the utilization of multiple emissions in the main fluorescence microscopy techniques. We first include a broad view of how fluorescence microscopy can benefit from the use of two or more emission channels. Then, we separately discuss how the use of multiple emission bands can enhance the most widely used fluorescence microscopy techniques, and highlight relevant examples of different applications, namely, labeling, characterization of the cellular structure and properties, and subcellular sensing. The different materials used in each fluorescence technique are presented and their strengths and weaknesses are discussed. Finally, we present our vision on future applications and perspectives of the use of multiple emissions.

In this review, we aim to give a different and broader view than previous reviews on the topic that focus on specific ratiometric sensors.[28–30] Also, we discuss a wider variety of applications and fluorescence microscopy techniques, some of which have not been reviewed before, on the topic of multichannel techniques.[31,32] As material scientists, we aim to give a description of the fundamentals of the different fluorescence microscopy techniques based on the properties of the materials they use. Finally, we do not restrict ourselves to dual-emission ratiometric sensing and imaging as we also discuss multilabeling and multiplexing applications.[33] We believe this review will encourage the fluorescence microscopy community to pursue the development of the field to reach more accurate and sensitive techniques through the design of multiple emitting fluorescent agents and new detection schemes to make of use of more than one emission and its benefits.

2. What Can Multiple Emissions Do for Fluorescence Microscopy?

In this section, we aim to compare multichannel microscopy techniques with conventional single-emission methods and give the reader a broad vision of the positive impact of the use of multiple detection channels before moving to the description of specific examples in different microscopy fluorescent techniques.

The basic strategy for fluorescence sensing is based on the comparison between the measured intensity at a particular instant with a reference value (usually the intensity at the beginning of the experiment or a control sample) to determine its evolution when the fluorescent agent is subjected to the presence of the analyte (specific protein, ion) or a change in the parameter (temperature, pH) under monitoring. These were sometimes called ratiometric techniques as the response is presented as the ratio of the measured intensity to the reference one. These single absolute emission (SAE) techniques (as they are going to be called hereinafter to distinguish them from actual ratiometric techniques that use two separate emissions to compute the ratio) present different well-known drawbacks. For example, they are very sensitive to changes produced on the probe's emission intensity by other factors than the presence of the analyte or the action of the parameter that is being monitored (e.g., variation in the excitation light intensity, photobleaching, changes in fluorescence probe concentration, or the existence of background fluorescence). This could lead to artifacts in the measurement which are sometimes difficult to identify and correct but must be accounted for.[34] As we are going to demonstrate in the following sections with specific examples, the use of multiple channels can improve the performance of fluorescence microscopy techniques and minimize the drawbacks of SAE methods.

For a better understanding of the comparison between the use of single or multiple emissions, **Figure 1** shows a schematic representation of a dual-channel technique. The total intensity from the sample is collected (Figure 1A) and then spectrally separated into two color channels (green, Figure 1B, and red, Figure 1C) using a beam splitter. The dual-channel technique allows one to image and distinguish different organelles of the cell simultaneously as each can be visualized in one of the channels (e.g., nucleus in green channel, Figure 1B.1, and actin filaments in the red channel, Figure 1C.1). For sensing, a dual-emitting sensor (probe) that emits in both channels (i.e., emits green and red light) can be placed in the intracellular medium and its emission used to sense a certain parameter with time (Figure 1B.2,C.2). To illustrate the benefits of the use of multiple

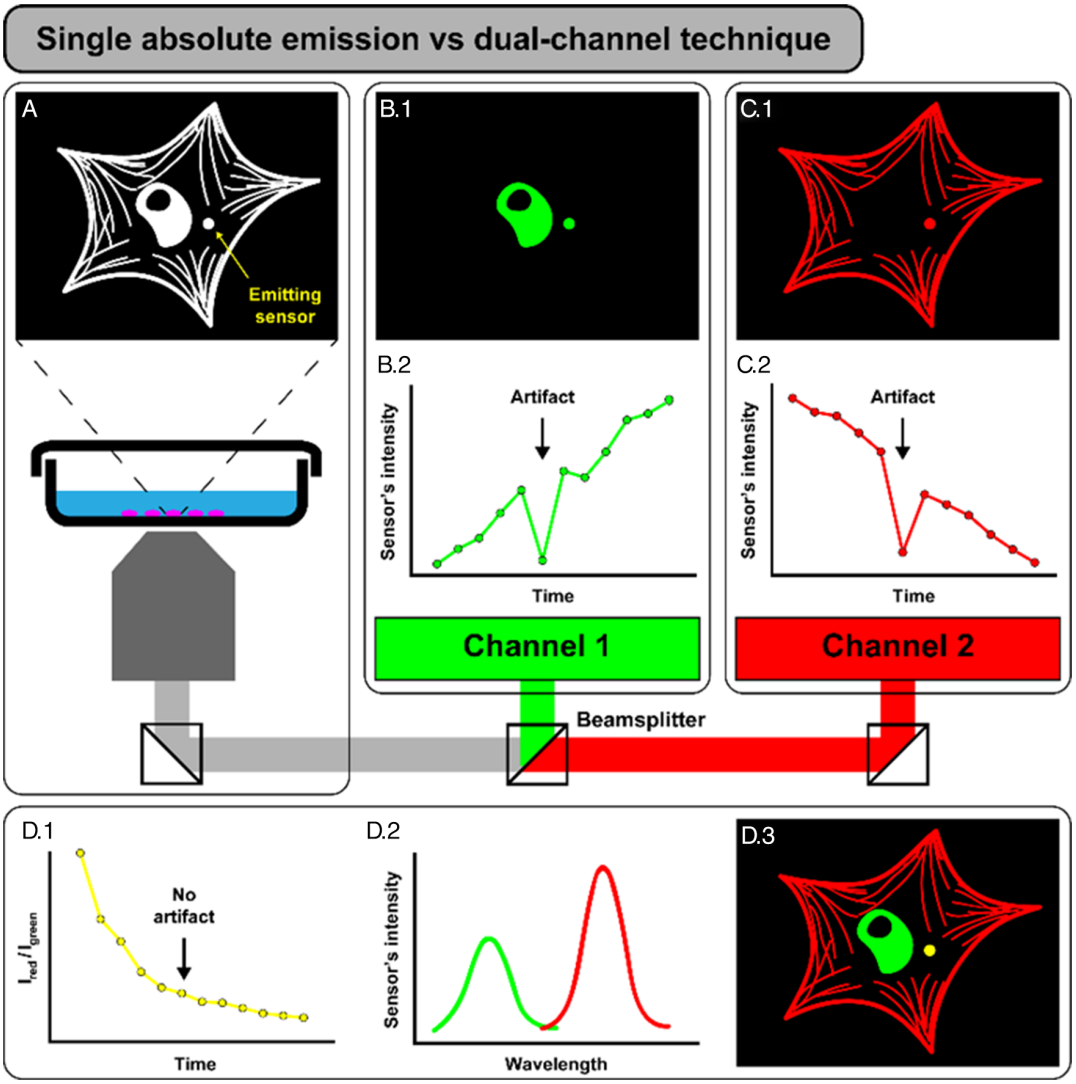

Figure 1. Single absolute emission versus dual-channel technique. A) The total emission from the sample is collected and spectrally separated using a beam splitter to create the two channels (B, green, and C, red). Each channel can image a different cellular organelle: B.1) nucleus in green channel, and C.1) acting filaments in red channel making use of distinct fluorescent labels. An emitting sensor (probe) located inside the cell presents emission in both channels whose intensity can be used to sense a certain intracellular parameter with time (B.2 and C.2). At some time instant, the probe's emission intensity presents a decrease that is not consistent with the overall trend of the signals. This artifact can be eliminated using the information of the two-color channels simultaneously (dual-channel technique, D) to compute the intensity ratio (D.1) that serves as the sensing signal to measure the intracellular parameter. The emission of the two channels can also be spectrally analyzed (D.2) to use all their spectral characteristics, not only the intensity. Finally, the merge of the two channels also allows the simultaneous imaging of the two intracellular regions (D.3).

emissions, we have simulated an artifact (marked with an arrow) in the emission of the probe that consists in a sudden well-localized reduction in the intensity detected in both channels. This could be caused, for example, by a decrease in the intensity of the excitation power.

The combination of both channels (dual-channel technique, Figure 1D) can eliminate the effect of the decrease in the measured intensity (that is clearly nonconsistent with the general trend). Instead of just utilizing the absolute emission from the sensor (i.e., total emission intensity or emission in a single channel, SAE technique), one can compute the intensity ratio between the two emissions, which eliminates the artifact, as shown in Figure 1D.1. In addition, in the dual-channel technique, the information of the two channels can be spectrally analyzed (Figure 1D.2) to use the spectral information of each emission separately. Moreover, the intensity of the two channels can be merged and visualized at the same time to generate a multicolor image (Figure 1D.3) to obtain better information on the cellular structure and see, for example, how those two subcellular components react to the parameter under study.

Usually, the utilization of multiple emissions requires small and easy-to-implement modifications of the typical experimental setup of fluorescence microscopes. For example, filters, polarizers, and beam dividers (as in the example of Figure 1) can

be used to select the spectral range or polarization state of the light of the different channels to be imaged in the same detector, even simultaneously.

Multiple emissions can be achieved using different emitting fluorophores excited in the same or separate spectral ranges.[35,36] However, it is preferable the use of a single emitter to minimize the cytotoxicity of multiple external agents. In addition, if the used fluorophores require different excitation sources, this will introduce uncertainties and experimental errors because each excitation source might present different fluctuations. The comparison between all these modalities of multichannel techniques and the SAE method is summarized in **Table 1**.

When measuring a single parameter, the combination of the response of two emission bands through the ratio can benefit the detection sensitivity of the reporter or spatial resolution of the imaging technique.[37,38] Self-reference sensors present at least one emission that does not change (or presents a weaker variation) in the presence of the analyte or when the parameter under monitoring varies.[39] Thus, one can account for changes in the sensing emission due to fluctuations in the excitation source, for example. Also, multiple coupled emissions that should respond in the same way and change synchronously can serve as a proof that the variations in the parameter to be measured are the sole cause of the luminescence changes.[40] This is critical to proof the reliability of intracellular measurements that is always under question due to the complex nature of the intracellular environment.

It is also worth noting that the use of multiple channels enabled the development of colorimetric or visual detection techniques.[41,42] These techniques measure the emission intensity of distinct color bands (e.g., blue, green, and red) that give rise to different color tones in the spectrum. The sensing technique is based on the change of apparent color of the signal due to the presence of a particular analyte. This variation can be the result of the change in the relative intensity of two emission bands,[43–45] or the spectral shift of a single band that moves to a distinct color channel.[46] This change in the apparent color can be detected by the naked eye, which gave rise to simple detection techniques that do not require a mechanic detector.

Once we have given this general overview, in the following sections we will give specific examples of the impact of the use of multiple emissions in different fluorescence microscopy techniques. A summary with some relevant examples can be found in **Table 2**.

3. Labeling Techniques

Identification, distinction, and tracking of individual cells in a microscope under regular illumination (i.e., using a lamp and a condenser) are challenging tasks especially in live cell assays because the cellular morphology (shape and size) fluctuates along time. In addition, morphology cannot be used to unambiguously identify intracellular changes (e.g., different level in protein expression), cell status (e.g., live round floating cells might look like dead cells), or cell type (e.g., normal vs cancerous cell). Furthermore, although the widely used differential interference contrast imaging improves the acquisition of cellular images,[47] the different cellular organelles are not easy to identify due to their small size, and similarities in composition, refractive index, and density. Fluorophores enable all this tasks, as it is evidenced by the multitude of fluorescence microscopy assays and tinctions that are commercially available. As we explain in this section, these studies can be further improved using multiple emission wavelengths (i.e., various labeling fluorophores or a single fluorophore with many emission bands) to, for example, label different cell organelles (**Figure 2**A.1) or to differentiate between cell populations (Figure 2A.2).

An example of regular practice that is performed with fluorophores is cell viability tests. These procedures are used to study, for example, the cytotoxicity produced by particles or to assess the action of treatments and drugs.[48] Nonviable cells are permeable to certain dyes, thus only they will be stained and easily distinguished from the viable cells.[49,50] Staining of both dead and live cells with dyes that emit at different wavelengths can allow one to directly quantify the amount of cells of each population by comparing the total intensity of each emission band.[51,52] Furthermore, apoptotic cells can be distinguished from dead and living cells using a ratiometric fluorescent probe whose two-band emission is highly sensitive to the lipid composition of the biomembranes. This makes it possible to sense the loss of the plasma membrane asymmetry occurring during the early steps of apoptosis.[53]

Beyond viability assays, multiple emission bands enable the detection, distinction, and tracking of numerous individual cells at the same time.[54–56] For example, the use of two labeling probes with different emission wavelengths (detected in two different channels) can serve to enhance the detection sensitivity and specificity of cytometry assays as only a positive response

Table 1. Comparison between SAE and multiple channel techniques. Different drawbacks and advantages of the use of a single or multiple emitters and one or several excitation sources are listed. Low, medium, and high are levels assigned in comparison between the five different cases. For example, the low toxicity attributed to the use of a single fluorophore is only in respect to the use of multiple emitters because the actual toxicity of the fluorophore depends on its characteristics.

Parameters to consider	SAE techniques		Multiple channel techniques		
Number of emitters	One	One	One	Multiple	Multiple
Number of excitation sources	One	One	Multiple	One	Multiple
Number of detection channels	One	Multiple	Multiple	Multiple	Multiple
Risk of toxicity	Low	Low	Low	High	High
Effect of excitation fluctuations	Medium	Low	High	Low	High
Effect of fluorescence efficiency	Low	Low	Low	Medium	High
Effect of concentration	Medium	Low	Low	High	High

Table 2. Multiple channel imaging and sensing. List of some important examples of fluorescent agents used in the different fluorescence microscopies techniques discussed in this review. SAE, single absolute emission; FRET, Förster resonance energy transfer; MRBF, molecular rotor-based fluorophore; FPA, fluorescent polarization anisotropy; SERRS, surface-enhanced resonance Raman scattering; STED, stimulated emission depletion.

Emitter type	Task	Fluorescent method	Ref.
Fluorescent protein	Thermal reading	Intensity (SAE)	[34]
Semiconductor nanoparticle	Cell tracking	Multiple emissions	[58]
Fluorescent protein, quantum dot, fluorescent dye, fluorescent antibody	Multilabeling	Multiple emissions	[64]
Rare-earth-doped particle, fluorescent protein	pH sensing	FRET	[120]
Fluorescent compound	Viscosity measurement	MRBF	[123]
Membrane probes	Membrane viscosity and packing density characterization	FPA	[127]
Fluorescent protein	Temperature sensing	Peak fraction analysis	[148]
Endogenous	Fatty acid structure characterization	Raman	[151]
Hybrid structure	Distinction between normal and cancer cells	Ratiometric SERRS	[157]
Fluorescent compound	Characterization of phase membrane	Lifetime	[148]
Organic fluorophore	High-resolution imaging	STED	[173]

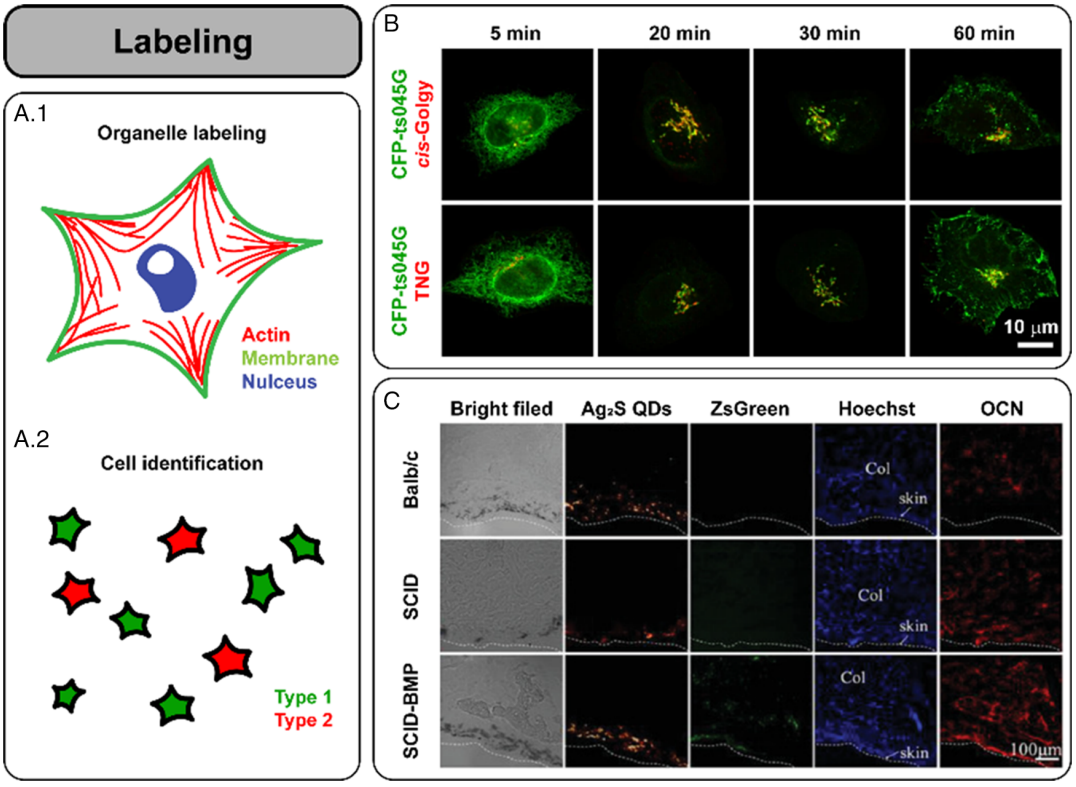

Figure 2. Multicolor labeling. Labeling with multiple colors allows to A.1) distinguish different cellular organelles, and A.2) differentiate between distinct cell populations. B) Colocalization of intracellular components. Cells fixed at various time points and then immunostained for markers of the *cis*-Golgi complex (top row) or the *trans*-Golgi network (TGN, lower row), both in red, for their colocalization with the transfected protein CFP-ts045G (green). The algorithm used to match the two-color channels allows to track CFP-ts045G along the secretory pathway: from the endoplasmic reticulum (5 min), through the Golgi complex (20 and 30 min), and toward the cell surface (60 min). Adapted under the terms and conditions of the Creative Commons Attribution license 2.0.[38] Copyright 2012, The Authors; licensee BioMed Central Ltd. C) Study of different parameters in a single assay for stem cell therapy studies. Bright field and fluorescent images of collagen scaffold sections obtained from Balb/c calvarial defect mice 30 days after transplantation with human mesenchymal stem cells (hMSCs). SCID indicates mice with immunodeficiency and BMP those that were treated with a bone morphogenetic protein. The green channel served to locate the living hMSCs among all the transplanted hMSCs showed in the yellow channel. The blue channel was used to locate both transplanted and host cells and the red emission served to assess the degree of osteogenic differentiation. Adapted with permission.[64] Copyright 2018, Wiley-VCH.

in both channels will be count as a hit.[57] In microscopy studies, the ability to study multiple cells individually and simultaneously would allow the obtention of relevant statistical results in a shorter time. Fikouras et al.[58] proposed that semiconductor nanodisk lasers internalized by cells could allow one to unequivocally tag more than 10^9 cells. These NPs present a very narrow emission whose spectral position depends on small changes in the nanodisk size. Thus, a single batch of slightly different sized NPs (i.e., with distinct emission wavelengths that can be distinguished thanks to their narrowness) could serve as barcodes to independently label single cells and track them during long periods of times. In this case, the emission of each nanodisk constitutes a single channel that is used to monitor a particular cell.

Detection of the spatial distribution of intracellular molecules or internalized particles within the cell volume and its organelles is required for numerous studies, such as to assess the tagging efficiency of functionalized particles or localize proteins within the cell volume. The usual strategy is labeling the entity to be localize (not needed if it fluoresces) and the cellular regions or organelles (e.g., nucleus, lysosomes, mitochondria) with commercial cell markers that emit at different colors. Then, the different color emissions are used to colocalize (find if there is spatial overlap between) the target and a particular cellular region using a visualization of the merged channels. As an example, the study of mitophagy can be facilitated through the dual staining of lysosomes and mitochondria for their colocalization.[59,60]

Different imaging analysis algorithms have been developed to quantify the correlation between the two-color channels in colocalization assays.[38,61–63] One example is the algorithm developed by Singan et al.[38] that allowed them to study the transport of a target protein along the first steps of the secretory pathway. They colocalized the emission of the transfected protein CFP-ts045G and the immunostained endoplasmic reticulum and the Golgi complex in cells fixed at different transport stages. They were able to reconstruct the transit of the protein through the organelles and localize it at their entrance and exit (Figure 2B), proving that the algorithm was able to detect relatively small changes in the distribution of the protein in those compact organelles. Their results agreed well with those obtained with biochemical techniques (normally used for these type of studies), but they were obtained more easily and even provide with quantitative information at cellular level.

Finally, multilabeling can facilitate the full understanding of biological processes that requires the simultaneous study of the role played by different agents or molecules, and cellular activity and state.[64,65] An example is stem cell therapy which requires to locate the transplanted cells and assess their survival and degree of differentiation. This would allow to fully understand the role of the stem cells in the therapeutic process and further improve the treatment. In this regard, multiple labels can be used for different purposes in a single assay. Huang et al.[64] studied the therapeutic capabilities of human mesenchymal stem cells (hMSCs), a type of cell present in the adult human bone marrow which contributes to the regeneration of multiple connective tissues.[66] They develop an essay (see Figure 2C) to 1) understand the role of both hMSCs and host cells in the regenerative process of Balb/c mice with a calvarial defect (top row); 2) study the effect of immunosuppression (SCID) on cell survival (middle row); 3) and determine the action of a bone morphogenetic protein (BMP), a key promoter of osteogenic differentiation (bottom row). To do so, they transduced hMSCs with a *Zoanthus* sp. green fluorescent protein (ZsGreen) gene and cultured them with near-infrared emitting Ag_2S quantum dots (QDs). The near-infrared emission of the QDs served them to locate the transplanted hMSCs (yellow channel, second column in Figure 2B), while the green emission of ZsGreen indicated the living hMSCs (green channel, third column). They also stained the cells with Hoechst (blue channel, forth column) to locate the nuclei of both hMSCs and host cells. Finally, they perform an immunofluorescence assay to locate osteocalcin (OCN, red channel, fifth column) that indicated the osteogenic differentiated cells. They could see an enhanced intensity in the green channel in the SCID group in comparison to the Balb/c group at 30 days after hMSCs's transplantation, which indicated that immunosuppression promoted the survival of hMSCs. Also, the larger red emission in SCID–BMP group in comparison to the other groups showed that the BMP enhanced the osteogenic differentiation of hMSCs. In addition, the colocalization of the near-infrared, green, and red emissions indicated that part of the transplanted hMSCs differentiated into osteogenic cells. In conclusion, in this study, the different reporters were used for different complementary purposes to fully assess the therapeutic process.

4. Sensing Techniques

The response of the fluorescent properties of dyes, proteins, and particles to an external stimulus has been extensively used for cellular sensing. As a result of a variation in the environment of the fluorophore, different fluorescent characteristics can vary (i.e., total emission intensity, the spectral position, the luminescence lifetime, and the polarization state), being each of them the basis of different microscopy techniques.

In this section, we explain how multiple emissions can be used to improve the capabilities of already established fluorescence sensing techniques that have been evolved toward being ratiometric. For example, simple strategies for the implementation of ratiometric pH sensing techniques use preexisting probes mixed together.[67] The ratiometric approach can minimize the effect of fluctuations produced by the ambient temperature or probe local concentration. However, as explained in Section 2, it is advantageous to use a single probe with multiple emissions. This strategy has been followed to characterize intracellular pH, ion concentration, or reactive oxygen species (ROS) production using ratiometric sensors based on fluorescent organic compounds,[42,44,68] luminescent particles,[69–74] and hybrid structures.[75–79] In addition, targeting ability can be achieved by combining the sensor with a specific cellular label or tagging molecule, whose emission can also be used for ratiometric sensing.[80–82]

Multiple emissions can be utilized to overcome the intrinsic limitations of certain sensors. For example, ROS probes are based on molecular compounds (e.g., boron dipyrromethene) that change their structure when they react (redox process) with these highly oxidative compounds. This produces a gradual variation in the probe emission with the largest fluorescent changes (maximum sensitivity) occurring when the molecule is completely modified. This process takes time to be completed

(tens of seconds); thus, most ROS probes fail to provide an accurate measurement with enough temporal resolution. Multichannel measurements can help in this regard as the luminescence changes of two independent probes can be detected and correlated to obtain an accurate, acquisition time-limited determination of the ROS concentration before the redox steady-state is reached by each probe.[74]

Finally, it is worth mentioning that the use of multiple emissions from the same emitter allows one to measure different parameters (e.g., temperature, pH, ROS) in the same assay using a single sensor.[83–89] In this same line, distinct compounds (e.g., different ROS) can be detected using a fluorescent sensor that emit at a different color in the presence of different analytes.[90–92] Moreover, the emitter can be designed to present emission bands in the visible and infrared ranges to be used for both in vitro and in vivo fluorescence molecular detection.

After this general introduction, in the following sections, we give specific examples of ratiometric sensing in different fluorescence microscopy techniques.[93]

4.1. Energy Transfer Techniques

Different fluorescent techniques have been developed using energy transfer-based sensors. The emission of these sensing agents is controlled by an energy transfer process (e.g., Förster resonance energy transfer [FRET]; luminescent radiative/resonance energy transfer) between two agents, the donor (absorbing unit) and the acceptor (emitting unit), which is highly sensitive to the donor–acceptor distance. The sensing capability of these techniques relies on the modulation of this process by the environment (e.g., presence of a targeted compound that modifies the donor–acceptor distance) and the consequent change in the emission intensity of the acceptor which is used as indicator. These techniques can make use of the strengths of multichannel methods if the emission of the donor is also exploited.[79,94,95]

Similarly, other techniques take advantage of the interaction of different fluorophores, such as absorption competition-induced emission,[96,97] where the fluorescence of the emitter is quenched by the presence of an absorbing agent, or aggregation-induced emission/quenching[98–101] that is based on the increase/decrease of the intensity emission or change in the lifetime due to the agglomeration of the fluorophores. Also, ratiometric sensors have been developed based on photoinduced electron-transfer effects,[102] or push–pull chromophores.[103]

FRET is the main example of the use of energy transfer-based techniques. It has made it possible incredible advances in fields such proteomics, signal transduction, diagnostics, and drug development, providing information unachievable by biochemical methods and conventional microscopies.[6] For example, as the FRET process can only occur at very short distances (<10 nm),[104] it is widely used to study molecular interactions that take places within proximity and it can serve to measure very small distances between molecules. For FRET-based detection, the differently emitting donor and acceptor can be functionalized with the antibody that specifically binds to the antigen to be detected.[105] In the absence of the antigen, just the donor emission is detected, and only when the two fluorescent markers bind to the antigen, the FRET-induced emission is detected. Similarly, ratiometric FRET can also be used to determine the binding affinity of two molecules each labeled with the donor or acceptor.[106] The presence or absence of FRET emission can be directly related to the attachment and detachment of the molecules. This can server, for example, to study the inhibiting ability of certain molecules to trigger the production of antioxidant enzymes for the treatment of oxidative-stress-related diseases.[107]

FRET between fluorophores can also be used to detect DNA damage. Yang et al.[108] developed a dual-emitting probe composed by Hoechst and naphtalimide dye to monitor the effect of a widely used anticancer drug. The complex presented a weak emission due to mutual quenching that recovered when the complex entered the nucleus and Hoechst bound to the DNA, which increased the distance between the fluorophores. In untreated cells, the ratiometric signal remained almost constant, while in treated cells, the emission of both fluorophores decreased as the DNA was progressively damaged by the drug, which released Hoechst molecules that reattached naphtalimide dye molecules.

This latter example relies on the presence of a biomolecule (DNA) to control the donor–acceptor distance. This approach can be further developed with the help of functional peptides that can additionally provide the fluorescent sensor with the capability of tagging or entering live cell with a specific characteristic.[109] For example, cancerous cells are known to overexpress certain proteins. Thus, the fluorescence reporters can be tailored to respond to the presence of these specific macromolecules using functional peptides.[110–113] As an example, Chan et al.[114] developed a nanocomposite formed by QDs attached to an upconverting nanoparticle (UCNP) which was able to change its emission color in the presence of matrix metalloproteinase 2 (MMP2), which is overexpressed in damaged and inflamed tissue, and in cells surrounding the invading front of metastatic tumors. The sensitivity of the nanocomposite emission to the presence of MMP2 was obtained through the functional peptide which linked the two types of NPs and allowed the FRET process to take place: the UCNPs emitted blue light under 800 nm excitation that was partially absorbed by the QDs which emitted red light (**Figure 3**A.1). When the link between the donor and acceptor was destroyed (digestion of the peptide link by the MMP2), the FRET process was interrupted and only the blue emission of the UCNPs could be detected (Figure 3A.2). The intensity ratio of the blue and red emission could be used to distinguish MMP2 overexpressing cells (label in blue) from cells that do not overexpress MMPs (label in red). In this case, the use of the donor emission, also as indicator, removes the possibility of a false-positive on the detection of MMP2 due a decrease in the acceptor emission intensity produced by, for example, a decrease in the excitation intensity.

Complex design and fabrication methods enable the construction of tumor-targetable, ratiometric FRET sensors based on aptamers that are nucleic acid analogues to antibodies that allow specific binding with high affinity and selectivity.[115–118] Kim et al.[115] proposed an easy synthetic method not used before to develop aptasensing platforms. They designed a FRET-based sensor to measure the intracellular adenosine triphosphate (ATP) level using an ATP-binding aptamer to which the donor

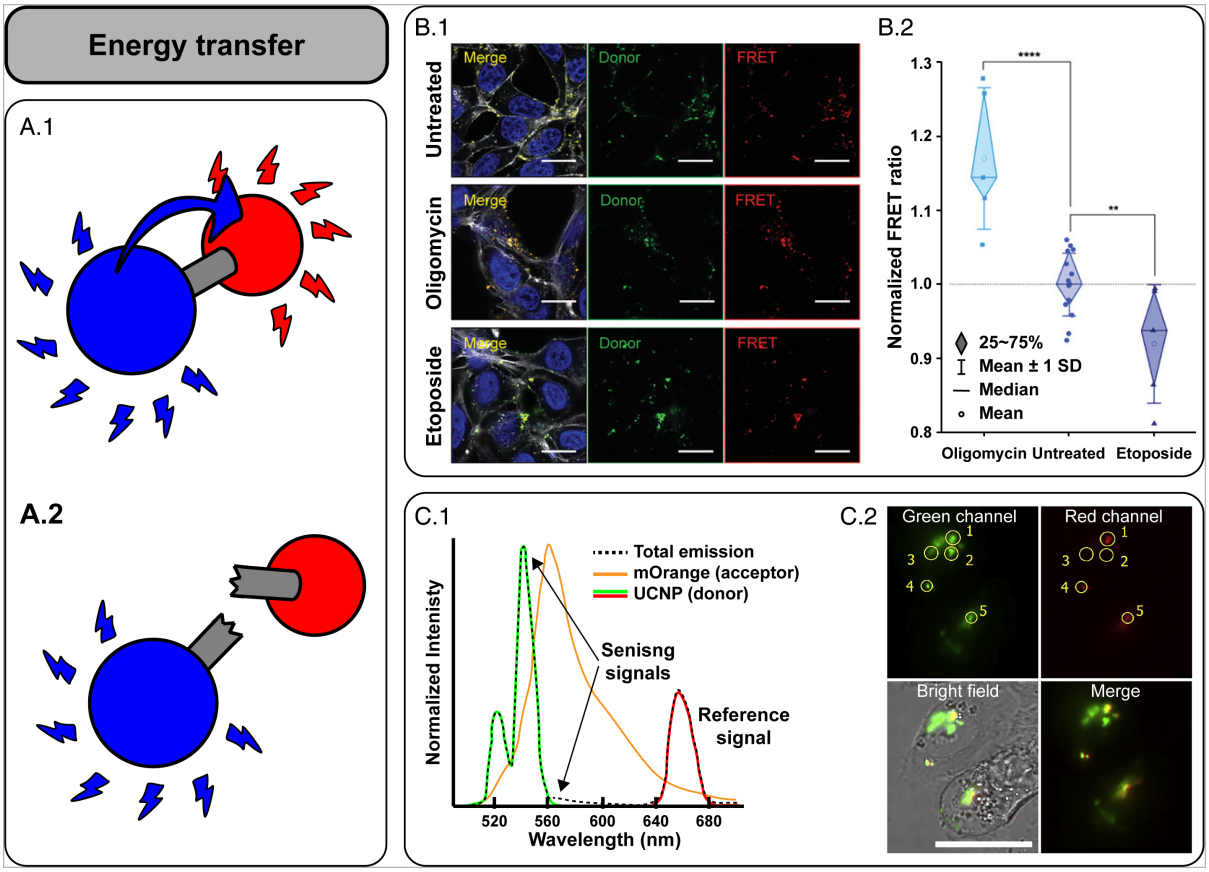

Figure 3. Energy transfer-based sensing. A) Schematic representation of a dual-emitting FRET sensor. A.1) When the donor (blue) and acceptor (red) are in proximity, the FRET process can take place and both fluorescent agents emit. A.2) When the link between them is broken, the donor cannot longer transfer the energy to the acceptor and only the donor emits. B) Dual-emitting aptasensor for APT sensing. B.1) The relative emission of the donor an acceptor differs in untreated cells and in cells treated with an inhibitor (etoposide) or inductor (oligomycin) of cytosolic ATP. B.2) The intensity ratio of the two channels serves to distinguish the three cell populations. Adapted under the terms and conditions of the Creative Commons Attribution license 4.0.[115] Copyright 2021, The Authors. Advanced Materials published by Wiley-VCH GmbH. C) Ratiometric pH sensing. C.1) The probe is composed by a UCNP (donor), and mOrange molecules (acceptor). Under 980 nm excitation, the construct presents a total emission (black dashed line) composed by the emission from the UCNP (540 and 655 nm, green and red bands) and mOrange molecules (small band at 566 nm). Emissions at 540 and 566 nm change with pH, thus are used for the ratiometric measurement, while emission at 655 nm is pH insensitive and used as a reference. C.2) The ratiometric technique can be used to determine the differences in pH of distinct cellular organelles form the change of color in the overlay image. Regions 1, 4, and 3 have a pH value of 7.2 associated to that of the cytosol, while regions 2 and 3 present an acidic pH (2.7 and 3.6, respectively) that can be associated to late endosomes or lysosomes. Adapted with permission.[120] Copyright 2020, Elsevier.

and acceptor were attached in proximity allowing the FRET process. For the sensing purpose, the acceptor partially occupied a specific portion of the ATP-binding aptamer. Thus, it will dislocate in the presence of the APT molecule that was revealed by a decrease in the FRET emission and a change in the ratiometric signal. To test their capability of monitoring intracellular ATP-level changes, they treated cells (Figure 3B.1) with drugs that either inhibit (etoposide) or induce (oligomycin) intracellular ATP production. For untreated cells, the intensity in both channels was almost the same. On the other hand, cells treated with the inhibitor showed a strong emission in the acceptor channel (red FRET channel), while in cells treated with drug that induces cytosolic ATP, the ration changed so that the donor channel (green) had a stronger emission. From the intensity ratio of the two emission channels, one can distinguish the three populations (Figure 3B.2).

FRET can also be utilized to generate multiemission pH sensors excited in the infrared to reduce photobleaching and phototoxicity and, this way, overcome the inherent drawbacks of the commonly used pH sensing probes based on fluorescent molecules and proteins (e.g., fluorescein and green fluorescent protein).[119] An example of this strategy is the combination of RE-doped UCNPs and pH sensitive fluorescent proteins.[120] Through a FRET process, infrared radiation can be used to excite the UCNP emission which is transferred to the fluorescent protein whose emission intensity depends on the environmental pH. The multiple emission bands characteristic of RE-doped particles can be used for two ratiometric measurements (Figure 3C.1). The first method is the regular dual-channel FRET-based sensing, where the donor emission (UCNP green band at 540 nm) is compared to the acceptor emission (band at 566 nm). The second method is a self-ratiometric

measurement that uses two emissions of the acceptor: the one involved in the FRET process (UCNP green band at 540 nm) and a second reference emission (UCNP red band at 640 nm) whose intensity is pH insensitive and unaffected by FRET. This way, self-ratiometry can account for changes in the whole acceptor emission (e.g., produced by fluctuations in the excitation) that can affect the FRET process, while the ratio between the acceptor and donor emissions presents the larger response to the environmental change and it is used for sensing. In addition, the ratiometric technique allows to map the intracellular pH from the change of color of the emission when detected in two channels (Figure 3C.2) and obtain an accurate measurement from the intensity ratio.

The distance dependence of the FRET efficiency can be harnessed to develop multiplexed sensors. Kaur et al.[121] developed a multiplexed DNA-based single molecule FRET sensor able to distinguish between specific nucleic acid sequences. It was composed by a DNA hairpin sandwiched between two short pieces of double-stranded DNA, each labeled with the donor or the acceptor fluorophore. The DNA harpin was maintained open by the action of a probe that kept the donor and acceptor at a distance that generated a low FRET efficiency (i.e., acceptor emission divided by the total emission of both emitters). In the presence of the target, the probe is displaced by the specific DNA sequence and the harpin closes increasing the FRET efficiency. They produced specific sensors creating different donor/acceptor distances by adding flanking thymine spacers of different lengths between the ends of the pieces of double-stranded DNA. Thus, each targeted molecule produced a different FRET efficiency level allowing multiplexed sensing.

Finally, ratiometric dual-channel sensors with the ability to simultaneously tag two cellular organelles and measure their properties would further help in the understanding of complex intracellular processes. As an example, ferroptosis (a pathway that regulates cell death) produces the accumulation of lipid-based ROS inside liquid droplets, which changes the polarity of these intracellular organelles. In addition, ferroptosis affects the structure and morphology of some cellular organelles, but not the nucleus, in contrast to other death pathways such as apoptosis. Thus, the monitoring of both the nucleus and liquid droplets would help to monitor ferroptosis and distinguish it from other death pathways. For this purpose, Wang et al.[103] developed a ratiometric dual-channel polarity sensor able to tag both the nucleus and liquid droplets at the same time. The dual probe was based on a push–pull chromophore (D–π–A, i.e., a strong electron donor, D, connected by a π-conjugating spacer to a strong electron acceptor, A) that presented two emission bands (green and red) whose relative intensity depended on the environment. The red emission enhanced when the probe was located in the nucleus and for increased polarity. Thus, it was used to locate the nucleus and track chromatin changes during ferroptosis (and distinguish the process from apoptosis), while the intensity ratio between the green and red bands was used to determine the changes in the polarity of the liquid droplets that fluoresced in green. This way, a single dual-emitting probe can be used to tag and characterize two cellular regions simultaneously using two-color channels.

4.2. Molecular Rotor-Based Techniques

Molecular rotor-based fluorophores (MRBFs) are fluorophores that rotate along specific bounds at excited state. Rotation quenches their emission as it acts as a nonradiative decay process (**Figure 4**A). The modulation of their emission can be harnessed to measure the properties of the environment such as viscosity. The emission of MRBFs enhances when the viscosity increases as the mobility is more restricted. Different emitting MRBFs with specific suborganelle targeting can be used to simultaneously monitor viscosity changes in two distinct organelles, even when they fuse together (e.g., interaction of lysosomes and mitochondria during mitophagy).[60,122] In addition, the chemical structure of the MRBFs can be tailored to control their response to the environmental viscosity and develop viscosity sensors with enhanced sensitivity in environments with distinct viscosity (i.e., low or high viscosity mediums).[37,123] Based on this idea, Ye et al.[123] developed a dual-channel viscosimeter for the distinction of misfolded oligomers (low viscosity) from insoluble aggregates (high viscosity) of proteins in live cells. They used two MRBFs, P2a and P2b, with spectrally separated emissions (green and red) and whose intensity was enhanced in high and low viscosity regions, respectively. They used these MRBFs to study the aggregation and accumulation of abnormally long polyglutamine (polyQ) expansion of the huntingtin proteins produced by a mutation associated to Huntington's disease.[124] Figure 4B shows how P2a (green channel) only detects the presence of dense insoluble aggregates of overexpressed Htt-110Q (case 2), while P2b (red channel) can image the former together with the low viscosity soluble oligomers generated in cells overexpressing Htt–46Q (case 1). In cells that normally express the protein, thus do not present agglomeration or accumulation, the MRBFs do not fluoresce (bottom row). This is an example of how two emissions can serve to distinguish intracellular elements with the same composition (i.e., protein), but with different physical characteristics (i.e., viscosity).

MRBFs can also be used to develop dual-emitting molecular sensors. For example, Mudliar et al.[125] developed a Thrombin sensor using a complex formed by the MRBF Thioflavin-T and Heparin. The fluorescence of Thioflavin-T redshifts (from the blue to the red) in the presence of Heparin when the two molecules aggregate (i.e., Heparin restricts the rotation of the MRBF producing the spectral change in the emission). Thrombin disrupts the complex due to its high affinity for Heparin, and Thioflavin-T recovers its blue emission. The use of two emission colors instead of the intensity at a single wavelength allows to detect Thrombin molecules unambiguously because no other factor than the interaction with that molecule could produce the spectral shift in the emission of the MRBF.

4.3. Techniques Based on Polarized Emission

Polarization-based techniques take advantage of the change in the polarization state of the emission to infer variations in the mobility of the fluorophore. For example, it is well known that the emission of RE-doped particles is highly polarized due to the effect of the crystalline structure of the host material. Thus, the spectral shape of the emission (i.e., relative intensity between two

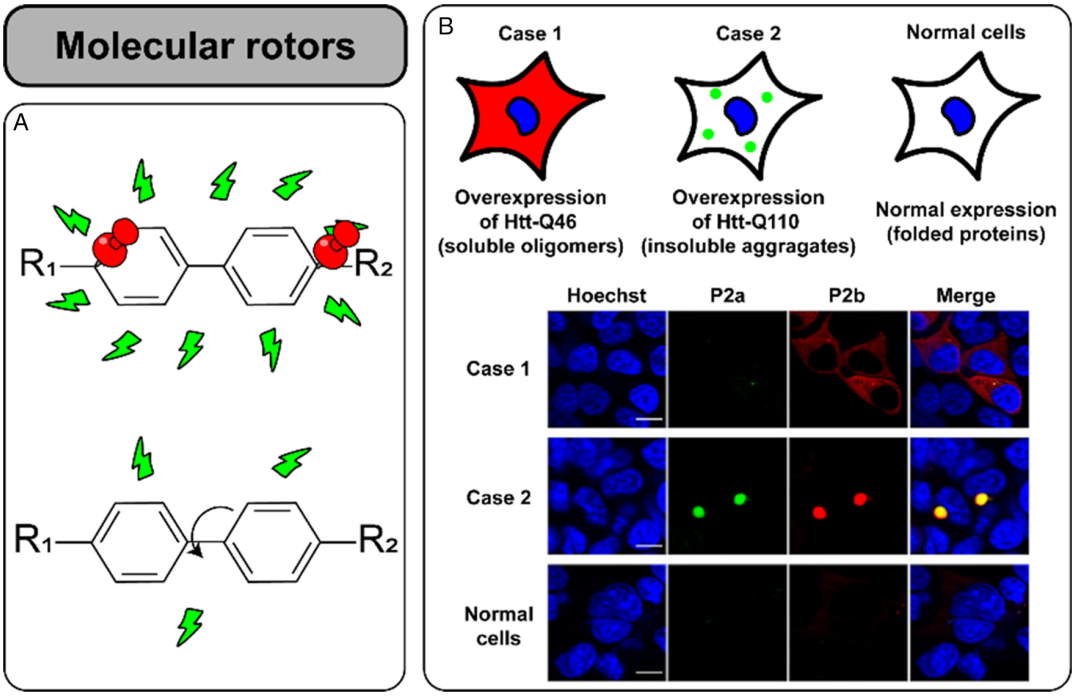

Figure 4. Molecular rotor-based sensing. A) The emission of molecular rotor-based fluorophores (MRBFs) is quenched when the molecule is able to rotate. B) Dual-emission viscosimeter based on two MRBFs for the detection of different viscosity regions produced by the agglomeration and accumulation of abnormally expressed proteins. The fluorescent sensors (P2a and P2b) emit in different spectral channels (green and red, respectively) and have different sensitivity to distinct viscosity ranges. They allow to clearly distinguish misfolded oligomers (case 1) from insoluble aggregates (case 2). The sensors do not emit when the proteins are normally folded (bottom row). Adapted with permission.[123] Copyright 2020, Wiley-VCH.

emission peaks or wavelengths that correspond to the two channels to be measured) depends on the orientation of the particle, which can be used to monitor its rotation and correlate it to the medium's viscosity. This strategy has been used to monitor intracellular viscosity changes induced during chemotherapy treatments.[126]

Similarly, molecular fluorophores emit linearly polarized light (**Figure 5**A.1) that becomes depolarized as the molecule emits at different angles while it rotates (Figure 5A.2). The depolarization degree or anisotropy of the emission can be measured from the ratio of the intensity detected in two orthogonally polarized channels. Anisotropy characterization and its use for the determination of the physical properties of the environment of the fluorophore are the basis of fluorescence polarization anisotropy (FPA) techniques.

Comparison of different anisotropy values has been used to detect viscosity and packing density changes of the cellular membrane produced by its interaction with signaling molecules.[127] More recently, FPA has been used to obtain a more accurate description of nanoregions within nonisotropic, heterogeneous systems environment, such as lipid droplet membranes, going beyond the concept of macroscopic viscosity.[128]

Soleimaninejad et al.[129] used an amine-reactive dye, TPE-Py-NCS, able to attach cytosolic proteins to map the macromolecular crowding effect. The variation in the crowding condition (agglomeration of proteins) affects the rotational freedom of the dye molecules producing a change in the fluorescence anisotropy. They mapped in real time the cytoplasmic crowding effect (Figure 5B.1) in cells subjected to osmotic stress. They showed how the FPA value distribution within the cytosol moved toward higher values (Figure 5B.2), indicating a reduction in the dye mobility produced by the tight packing of the proteins.

Apart from viscosity, another important parameter that directly influences the mobility of the fluorophore is temperature. It is directly related to the Brownian fluctuations and affects the viscosity. This can be exploited to develop FPA nanothermometers based on fluorescence molecules such as fluorescent proteins,[130,131] dyes,[132] proteins conjugated with dyes,[132,133] and DNA labeled with intercalated dyes.[134] As for MRBFs (see Section 4.2), the fluorescent agent can be engineered to enhance its response to temperature and measure changes in this parameter through the variation in the sensor's mobility using FPA.[132] As Donner et al. described,[130] the maximum sensitivity is found when the lifetime of the fluorescent probe is in the same range of its rotational lifetime. Utilizing the green fluorescent protein (GFP) as anisotropy-based nanothermometers (ABNTs), they mapped the intracellular temperature of HeLa cancer cells.[130] Likewise, this technique was applied utilizing the complex GFP tagged to the enzyme glutamic acid decarboxylase as ABNTs in GABAergic neurons.[131]

4.4. Fluorescence Thermometry

Fluorescence thermometric techniques are tightly related to other fluorescent sensing methods as they rely on the thermal

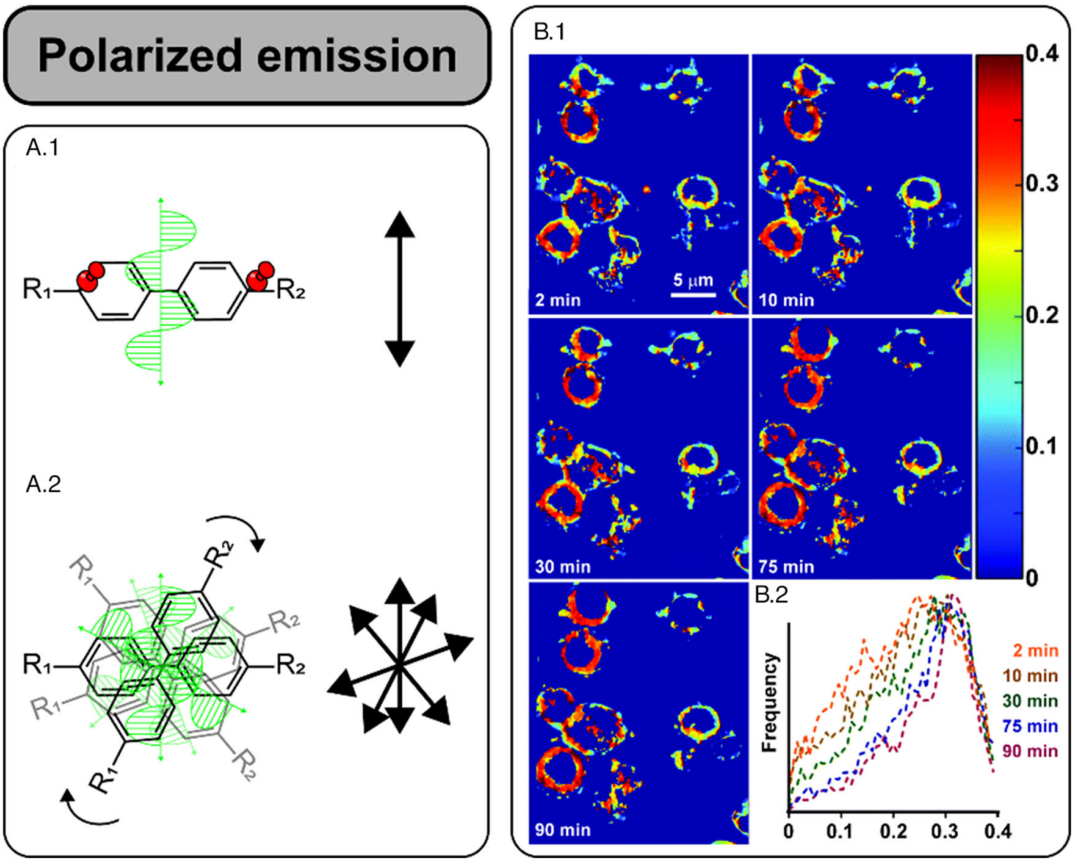

Figure 5. Polarized emission-based sensors. A) The emission of molecular fluorophores is linearly polarized (A.1) and becomes depolarized as the molecule emits at different angles while it rotates (A.2). B) Polarization anisotropy serves to map the cytoplasmic crowding effect in cells subjected to osmotic stress. B.1) Anisotropy maps for different time instant. Large anisotropy values (low molecular rotational motion) indicate regions of higher protein packing. B.2) The anisotropy distribution displaces to lager anisotropy values as the crowding effect increases. Adapted with permission.[129] Copyright 2017, The Royal Society of Chemistry.

changes produced in the intensity, spectral position, lifetime, or polarization state (see Section 4.3) of the emission of luminescent organic molecules and particles.[135–137] Thus, here we only highlight certain aspects of the use of multiple emissions for thermosensing and the materials involved.

In ratiometric themometry, the combination of the response of two emission bands from the same emitter can benefit the sensitivity and resolution of the probe. For this, RE-doped particles are the preferred choice as they present multiple emission bands with different sensitivities to temperature changes. For example, the two thermally coupled, green emission bands of erbium ions present opposite behavior with temperature, thus their intensity ratio can be used to measure temperature in specific intracellular organelles.[138] The sensitivity of thermally coupled level-based thermometers is directly related to the energy difference between the emitting levels; thus, they usually suffer from low sensitivity due to the restriction of small energy gap. To overcome this limitation, other thermally sensitive energy transfer processes have been investigated to achieve better thermal resolutions with RE ions.[139,140] In addition, alternative materials have been engineered to present multiple emission bands, on their own or in synergy, for ratiometric thermometry, such as fluorescent proteins,[141] organic dyes,[142,143] nanopolymers,[144] quantum dots,[145,146] or gold nanoparticles.[147]

A recent example of ratiometric thermometry makes use of the spectral shift produced in the emission of GFP.[148] The authors used a technique called peak fraction analysis that is based on the difference between the integrated intensity in two spectral rages of the GFP emission band. As the emission peak shifts toward larger wavelengths, the relative intensity between the two spectral regions changes. They divided the difference between the emission intensities by the total integrated emission to account for the decrease in the GFP emission due to the change in temperature. In this way, the spectral shift of the emission peak produced by temperature can be obtained without the need of a precise determination of its central position. Using this technique, they obtain a relative thermal sensitivity one order of magnitude larger than that of GFP using FPA method.

4.5. Raman Spectroscopy

Raman spectroscopy uses the inelastic scattering of monochromatic photons (laser radiation) to extract detailed information of the chemical composition of the sample. The energy difference

between the incident photon and the Raman scattered photon corresponds to the energy of specific molecular vibrations. Thus, the Raman spectrum is a fingerprint of the molecules that compose the sample (**Figure 6**A). Raman spectroscopy has proven its reliability as a label-free diagnostic tool as it is able to specifically identify biomolecules with high sensitivity and give information on the alteration of molecular signatures at the cellular level or in tissues.[149] This technique (and its modalities, e.g., surface-enhanced Raman scattering [SERS]; surface-enhanced resonance Raman scattering [SERRS]; stimulated Raman scattering [SRS]) can benefit from the use of multiple emissions because each of the Raman peaks can be considered as a color channel. As an example, normal Raman cannot provide quantitative information on the protein carbonyl levels, associated to protein oxidation, because the protein Raman spectrum is dominated by the spectral features of aromatic amino acids and the protein skeletal modes which are not affected by oxidation. To solve this issue, Zhang et al.[150] conjugated protein carbonyl with dinitrophenyl hydrazine (DNPH), a label commonly used in spectrophotometric and immunoassay-based methods. The Raman spectrum of the oxidated protein conjugated with DNPH presented the spectral features of the oxidated protein alone plus those of DNPH. They used the intensity ratio between one characteristic Raman peak of DNPH and another from the oxidated protein to accurately determine the carbonyl levels. This is one of the first examples of ratiometric Raman which is currently a common practice for detection, quantification, and structural characterization of biomolecules.[151–154]

Although Raman is a label-free technique, it can benefit from the use of specific markers, as DNPH in the previous example. This is especially relevant for SERS, SERRS, or SRS techniques,[155] where a metallic particle can be used to enhance the Raman signal that is usually very weak (i.e., less than 1 in 10^8 of incident photons undergoes Raman scattering).[149] As an example, specific ratiometric sensors for SRS can be developed for the detection of intracellular pH.[156]

Raman markers can also be designed to present distinctive Raman spectra that can be easily distinguished, in comparison to the bulk Raman spectra of a sample that is composed by the superposition of the different spectrum of each molecule. This allows multiplexing because each of the markers can target a specific biomolecule that can be detected using the specific Raman spectrum of the marker. This strategy has been used for the detection and differentiation between cell lines, especially in the detection of cancerous cells.[157–161]

In an early example, Pallaoro et al.[157] developed a multiplexed ratiometric SERRS method for the distinction between normal and cancerous prostate cells. They used two Raman markers composed by polymer-encapsulated silver particles (Figure 6B.1), each labeled with a unique Raman reporter molecule (i.e., with distinct Raman spectrum, Figure 6B.2). Each of the Raman markers was functionalized with either a receptor-specific peptide, or a general cell penetrating peptide (CPP). While the first

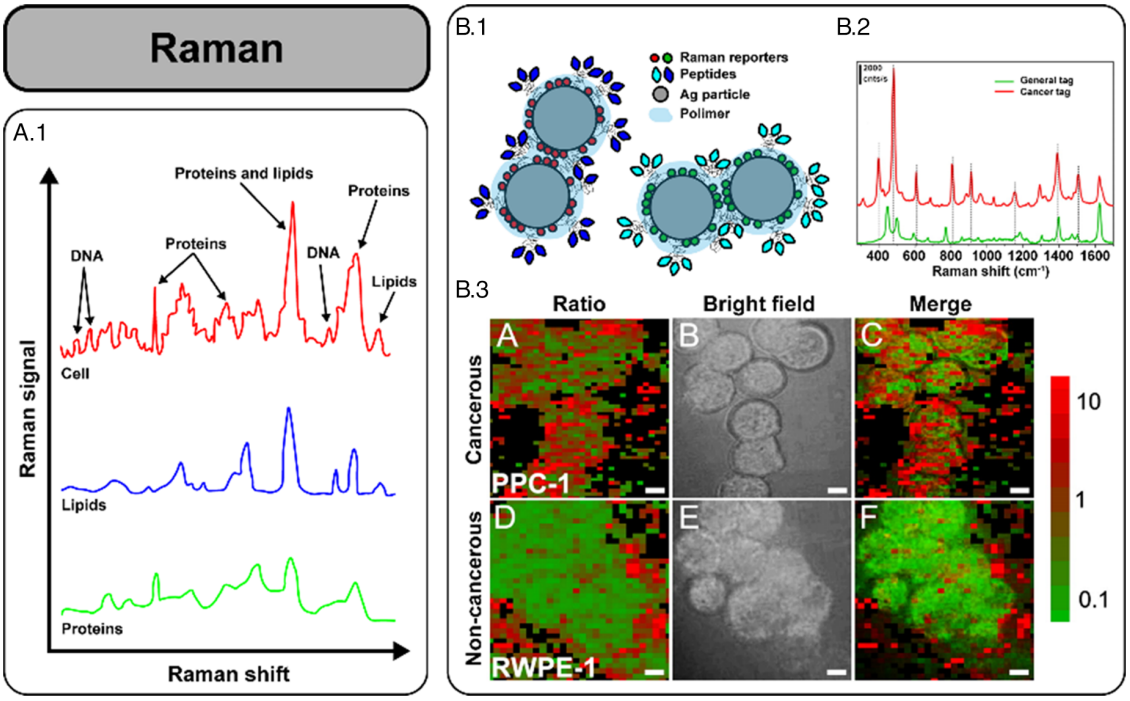

Figure 6. Raman sensors. A) The Raman spectrum of a cell is the superposition of all the spectra of each of the biomolecules that compose it (e.g., DNA, proteins, lipids). Each of these molecules has a unique spectrum that can be considered as their fingerprint. B) Cell identification using Raman markers. B.1) The two Raman markers are constructs of two silver particles each coated with a different Raman reporter and a distinct peptide: one able to tag cancer cells (red), while the other can enter both cancerous and normal cells (green). B.2) The markers can be distinguished thanks to their distinct Raman spectra provided by the two different Raman reporters. B.3) Point scanning maps of the ratio between the Raman signal of the two markers (red to green ratio). The green signal is present in both cell types, while the red signal is mostly present in cancer cells giving a high value of the ratio. Adapted under the terms and conditions of the Creative Commons Attribution license 4.0.[157] Copyright 2011, The Authors, published by the National Academy of Sciences.

type of Raman marker (red) can only tag cancerous cells, both normal and cancer cells internalized the CPP markers (green), which were used as a positive control. They used the ratio between the amount of signal detected for each Raman marker (red marked divided by green marker) to construct 2D maps of the distribution of the peptides in cells and thus distinguish between the two cell types (Figure 6B.3). As only cells displaying both types of markers counted as positive hit, they managed to reduce the uncertainty in the quantitative measurement that can result from, for example, variability in focal plane, changes in turbidity, cell concentration, or short measurement time.

4.6. Fluorescence Lifetime Microscopy

Although fluorescence lifetime microscopy techniques do not suffer from the main drawbacks of SAE methods, they can still benefit from then use of multiple emissions. Thus, although in this review we are focused on the use on the spectral and intensity characteristics of the fluorescent emission, we also want to briefly discuss the use of multiple channels in fluorescence lifetime microscopy. In this case, separate channels can be different lifetime intervals.[162] For example, dyes are known to have a fluorescence lifetime of the order of nanoseconds, while the emission of RE-doped particles can be pushed to be close to 1 ms. The distinction between the lifetime of the probe and that of the autofluorescence of the sample (in the order of nanoseconds) can be used in time-gated experiments to reduce the background noise and enhance the resolution.[163] For multiplexing, particles can be engineered to present distinct lifetime, avoiding the problem of spectral overlapping of different color emissions.[164] In addition, lifetime could help developing heavily multiplexed assays,[165] enabling multiparameter assays for better understanding of biological processes.

Another interesting aspect of the lifetime is that it is highly dependent on the environment of the fluorophore. Different nonradiative deexcitation processes can compete with the radiative deexcitation path and modify the fluorescence lifetime. For example, analogously to the use of two emissions from the same probe that behave differently depending on the environmental conditions, the mean and long components of the lifetime of the chemical compound F2N12S can be used to distinguish ordered and disordered phases of lipid membranes.[148]

5. Super Resolution Fluorescence Microscopy Techniques

The implementation of the use of multiple channels in already established super-resolution microscopy techniques allows to perform all the abovementioned tasks (e.g., multiplexing, ratiometric sensing) with increased imaging resolution. One can find examples of the use of multiple emissions in stochastic optical reconstruction microscopy (STORM),[166–168] fluorescence photoactivation localization microscopy,[169,170] ground state depletion microscopy followed by individual molecule return,[171,172] stimulated emission depletion (STED) microscopy,[173–175] or super-resolution optical fluctuation imaging.[176] Even novel multiemitting probes have been specially developed for ratiometric fluorescence sensing in STED microscopy.[175] Dual-color super-resolution techniques have, for example, enabled the localization at the nanoscale of particular proteins in the mitochondria membrane using STED or to measure the distributions of synaptic proteins with nanometer precision using STORM.[173,177]

The combination of super-resolution and the numerous advantages of the use of multiple emissions could give rise to novel and improved methods that could even enable the fast acquisition of highly detailed images of large specimens in three dimensions.

6. Conclusions

In this review, we have discussed how fluorescence microscopy can benefit from the use of more than just one emission. Multilabeling permits the visualization of different parameters or cellular regions at the same time and the localization of biomolecules with high spatial resolution. In addition, multiple emitting channels allow the construction of ratiometric sensors that could even be self-referenced; thus, they are not affected by experimental artifacts such as fluctuations in the excitation radiation or differences in the probe concentration.

Multiple emissions can be produced by just one or different emitting agents. In the latter case, many approaches get advantage of the interaction of different fluorescent agents through energy transfer processes. This requires a judicious design of the luminescent agents (e.g., the emission of the donor must match the absorption band of the acceptor). For this reason, there is a strong and symbiotic relation between these novel microscopy techniques and the development of new synthetic methods that can even have an impact in other research fields.

Despite all the discussed advantages and promising future applications, the field requires the standardization of the microscopy sensing probes and techniques, especially when dealing with the analysis of multiple parameters at the same time. Due to the complexity of the intracellular medium, the problem under study has multiple variables that entail numerous effects that can be simultaneously influencing the sensor's feedback. Thus, unequivocal interpretation of the results is not always easy and might be subjected to bias. As an example, the detection of intracellular viscosity should be accompanied by a thorough analysis of other intracellular parameters (e.g., temperature) that could be, or in fact are, also affecting the emission of the sensor. In addition, the field needs to establish a standardized method to compute the sensitivity and reliability of the microscopy techniques as it is done in other analytic fields. This will help to make a fair comparison between all the different sensors in the literature. In our opinion, fluorescence microscopy will not be able to evolve if these issues are not seriously considered.

Acknowledgements

This research was funded by the Science and Innovation Spanish Ministery (grant nos. RTI2018-101050-J-I00, PID2019-106211RB-I00, and EIN2020-112419. P.R.S. is grateful for a Juan de la Cierva Incorporación scholarship (IJC2019-041915-I).

Conflict of Interest

The authors declare no conflict of interest.

Keywords

biomedical applications, fluorescence microscopy, intracellular sensing, multichannel, multiplexing, ratiometric sensing

Received: June 30, 2021
Revised: November 29, 2021
Published online: January 5, 2022

[1] World Health Organization. Regional Office for the Eastern Mediterranean, **2005** Fluorescence microscopy for disease diagnosis and environmental monitoring.
[2] A. Ojha, S. Banik, S. K. Melanthota, N. Mazumder, *Lasers Med. Sci.* **2020**, *35*, 1431.
[3] S. M. Zunder, H. Gelderblom, R. A. Tollenaar, W. E. Mesker, *Crit. Rev. Oncol. Hematol.* **2020**, *151*, 102907.
[4] M. Sunder, N. Acharya, S. Nayak, N. Mazumder, *Appl. Spectrosc. Rev.* **2021**, *56*, 764.
[5] K.-T. Jin, J.-Y. Yao, X.-J. Ying, Y. Lin, Y.-F. Chen, *Curr. Top. Med. Chem.* **2020**, *20*, 2737.
[6] C. Ma, W. Sun, L. Xu, Y. Qian, J. Dai, G. Zhong, Y. Hou, J. Liu, B. Shen, *J. Mater. Chem. B* **2020**, *8*, 9642.
[7] M. Won, M. Li, H. S. Kim, P. Liu, S. Koo, S. Son, J. H. Seo, J. S. Kim, *Coord. Chem. Rev.* **2021**, *426*, 213608.
[8] Q. Xia, S. Feng, J. Hong, G. Feng, *Talanta* **2021**, *228*, 122184.
[9] T. G. Iversen, T. Skotland, K. Sandvig, *Nano Today* **2011**, *6*, 176.
[10] M. Jordan, A. Schallhorn, F. M. Wurm, *Nucleic Acids Res.* **1996**, *24*, 596.
[11] B. Zhitomirsky, H. Farber, Y. G. Assaraf, *J. Cell. Mol. Med.* **2018**, *22*, 2131.
[12] Y. Li, M. Gecevicius, J. Qiu, *Chem. Soc. Rev.* **2016**, *45*, 2090.
[13] N. Liu, X. Chen, X. Sun, X. Sun, J. Shi, *J. Nanobiotechnol.* **2021**, *19*, 1.
[14] Y.-Q. Liu, L.-Y. Qin, H.-J. Li, Y.-X. Wang, R. Zhang, J.-M. Shi, J.-H. Wu, G.-X. Dong, P. Zhou, *Nanomedicine* **2021**, *16*, 2207.
[15] A. A. Ansari, A. K. Parchur, N. D. Thorat, G. Chen, *Coord. Chem. Rev.* **2021**, *440*, 213971.
[16] I. A. Vorobjev, E. P. Rafalovskaya-Orlovskaya, A. A. Gladkih, D. M. Potashnikova, N. S. Barteneva, *Cell Tissue Biol.* **2011**, *5*, 321.
[17] S. Lee, Y. Sun, Y. Cao, S. H. Kang, *TrAC - Trends Anal. Chem.* **2019**, *117*, 58.
[18] Y. An, Y. Ren, M. Bick, A. Dudek, E. Hong-Wang Waworuntu, J. Tang, J. Chen, B. Chang, *Biosens. Bioelectron.* **2020**, *154*, 112078.
[19] H. Ali, S. Ghosh, N. R. Jana, *WIREs Nanomed. Nanobiotechnol.* **2020**, *12*, 1617.
[20] U. Cho, J. K. Chen, *Cell Chem. Biol.* **2020**, *27*, 921.
[21] V. Gubala, G. Giovannini, F. Kunc, M. P. Monopoli, C. J. Moore, *Cancer Nanotechnol.* **2020**, *11*, 1.
[22] S. Yang, Y. Li, *WIREs Nanomed. Nanobiotechnol.* **2020**, *12*, 1603.
[23] N. Gözübenli, E. Yasun, N. Dilsiz, *Turk. J. Biol.* **2017**, *41*, 673.
[24] Y. Fu, G. Zeng, C. Lai, D. Huang, L. Qin, H. Yi, X. Liu, M. Zhang, B. Li, S. Liu, L. Li, M. Li, W. Wang, Y. Zhang, Z. Pi, *Chem. Eng. J.* **2020**, *399*, 125743.
[25] A. P. Demchenko, *Introduction To Fluorescence Sensing*, Springer **2009**.
[26] A. S. Klymchenko, *Acc. Chem. Res.* **2017**, *50*, 366.
[27] J. T. C. Liu, M. W. Helms, M. J. Mandella, J. M. Crawford, G. S. Kino, C. H. Contag, *Biophys. J.* **2009**, *96*, 2405.
[28] X. Pei, Y. Pan, L. Zhang, Y. Lv, *Appl. Spectrosc. Rev.* **2021**, *56*, 324.
[29] R. Zhang, F. Yan, Y. Huang, D. Kong, Q. Ye, J. Xu, L. Chen, *RSC Adv.* **2016**, *6*, 50732.
[30] H. Jin, M. Yang, Z. Sun, R. Gui, *Coord. Chem. Rev.* **2021**, *446*, 214114.
[31] X. Huang, J. Song, B. C. Yung, X. Huang, Y. Xiong, X. Chen, *Chem. Soc. Rev.* **2018**, *47*, 2873.
[32] D. Andina, J. C. Leroux, P. Luciani, *Chem. A Eur. J.* **2017**, *23*, 13549.
[33] Y. Zhang, D. Hou, Z. Wang, N. Cai, C. Au, *Polymers* **2021**, *13*, 2540.
[34] Y. Kamei, M. Suzuki, K. Watanabe, K. Fujimori, T. Kawasaki, T. Deguchi, Y. Yoneda, T. Todo, S. Takagi, T. Funatsu, S. Yuba, *Nat. Methods* **2008**, *6*, 79.
[35] G. L. Hong, H. H. Deng, H. L. Zhao, Z. Y. Zou, K. Y. Huang, H. P. Peng, Y. H. Liu, W. Chen, *J. Pharm. Biomed. Anal.* **2020**, *189*, 113480.
[36] Y. Xu, H. Yu, L. Chudal, N. K. Pandey, E. H. Amador, B. Bui, L. Wang, X. Ma, S. Deng, X. Zhu, S. Wang, W. Chen, *Mater. Today Phys.* **2021**, *17*, 100328.
[37] J. Ordóñez-Hernández, A. Jiménez-Sánchez, H. García-Ortega, N. Sánchez-Puig, M. Flores-Álamo, R. Santillan, N. Farfán, *Dyes Pigm.* **2018**, *157*.
[38] V. R. Singan, T. R. Jones, K. M. Curran, J. C. Simpson, *BMC Bioinf.* **2011**, *12*, 1.
[39] M. G. Walker, V. Ramu, A. J. H. M. Meijer, A. Das, J. A. Thomas, *Dalton Trans.* **2017**, *46*, 6079.
[40] M. Schubert, L. Woolfson, I. R. M. Barnard, A. M. Dorward, B. Casement, A. Morton, G. B. Robertson, P. L. Appleton, G. B. Miles, C. S. Tucker, S. J. Pitt, M. C. Gather, *Nat. Photonics* **2020**, *14*, 452.
[41] A. Bigdeli, F. Ghasemi, S. Abbasi-Moayed, M. Shahrajabian, N. Fahimi-Kashani, S. Jafarinejad, M. A. Farahmand Nejad, M. R. Hormozi-Nezhad, *Anal. Chim. Acta* **2019**, *1079*, 30.
[42] S. D. Padghan, L. C. Wang, W. C. Lin, J. W. Hu, W. C. Liu, K. Y. Chen, *ACS Omega* **2021**, *6*, 5287.
[43] D. Hu, T. Zhang, S. Li, T. Yu, X. Zhang, R. Hu, J. Feng, S. Wang, T. Liang, J. Chen, L. N. Sobenina, B. A. Trofimov, Y. Li, J. Ma, G. Yang, *Nat. Commun.* **2018**, *9*, 362.
[44] S. Liu, D. Yang, Y. Liu, H. Pan, H. Chen, X. Qu, H. Li, *Sens. Actuators, B Chem.* **2019**, *299*, 126937.
[45] J. Fan, E. Wu, J. Dong, R. Zhu, M. Li, J. Gao, H. Han, L. Ding, *Colloids Surf. A* **2021**, *616*, 126299.
[46] P. Ravichandiran, A. Boguszewska-Czubara, M. Masłyk, A. P. Bella, S. A. Subramaniyan, P. M. Johnson, K. S. Shim, H. G. Kim, D. J. Yoo, *ACS Sustainable Chem. Eng.* **2019**, *7*, 17210.
[47] H. E. Rosenberger, In *Interpretive Techniques For Microstructural Analysis*, Springer, Boston, MA, **1977**, pp. 79–104.
[48] C. Elamathi, A. Madankumar, W. Kaminsky, R. Prabhakaran, *Inorg. Chim. Acta* **2019**, *496*, 119039.
[49] X. Qie, M. Zan, L. Li, P. Gui, Z. Chang, M. Ge, R. S. Wang, Z. Guo, W. F. Dong, *Colloids Surf. B* **2020**, *191*, 110987.
[50] H. J. Phillips, In *Tissue Culture* (Eds.: P. F. Kruse; M. K. B. T.-T. C. Patterson), Academic Press, Cambridge **1973**, pp. 406–408.
[51] K. H. Jones, J. A. Senft, *J. Histochem. Cytochem.* **1985**, *33*, 77.
[52] J. Lee, G. D. Lilly, R. C. Doty, P. Podsiadlo, N. A. Kotov, *Small* **2009**, *5*, 1213.
[53] V. V. Shynkar, A. S. Klymchenko, C. Kunzelmann, G. Duportail, C. D. Muller, A. P. Demchenko, J. M. Freyssinet, Y. Mely, *J. Am. Chem. Soc.* **2007**, *129*, 2187.
[54] M. Xie, L. Guo, S. Xing, S. Cao, Z. Zhao, K. Liang, J. Li, S. Luo, Y. Zhang, L. Wang, *Chem. Commun.* **2021**, *57*, 11318.

[55] P. Rees, J. W. Wills, M. R. Brown, J. Tonkin, M. D. Holton, N. Hondow, A. P. Brown, R. Brydson, V. Millar, A. E. Carpenter, H. D. Summers, *Nat. Methods* **2014**, *11*, 1177.
[56] A. Dey, Z. Ni, M. S. Johnson, L. M. Sedger, *J. Immunol. Methods* **2021**, *491*, 112988.
[57] I. Altamore, L. Lanzano, E. Gratton, *Meas. Sci. Technol.* **2013**, *24*, 065702.
[58] A. H. Fikouras, M. Schubert, M. Karl, J. D. Kumar, S. J. Powis, A. Di Falco, M. C. Gather, *Nat. Commun.* **2018**, *9*, 4817.
[59] H. Xu, Y. Bu, J. J. Wang, M. Qu, J. Zhang, X. Zhu, G. Liu, Z. Wu, G. Chen, H. Zhou, *Sens. Actuators, B Chem.* **2021**, *330*, 129363.
[60] Q. Chen, H. Fang, X. Shao, Z. Tian, S. Geng, Y. Zhang, H. Fan, P. Xiang, J. Zhang, X. Tian, K. Zhang, W. He, Z. Guo, J. Diao, *Nat. Commun.* **2020**, *11*, 1.
[61] Y. Qiang, J. Y. Lee, R. Bartenschlager, K. Rohr, In *Proc. Int. Symp. on Biomedical Imaging*, IEEE Computer Society, Melbourne, Australia **2017**, pp. 646–649.
[62] H. Wang, J. Suo, L. Bian, Q. Dai, W. Zhang, Z. Zhang, Q. Dai, Q. Dai, *Opt. Lett.* **2021**, *46*, 5477.
[63] Z. A. Farsani, V. J. Schmid, *Int. J. Biostat.* **2021**, *17*, 165.
[64] D. Huang, S. Lin, Q. Wang, Y. Zhang, C. Li, R. Ji, M. Wang, G. Chen, Q. Wang, *Adv. Funct. Mater.* **2019**, *29*, 1806546.
[65] L. Deng, X. Huang, C. Dong, J. Ren, *Analyst* **2021**, *146*, 2581.
[66] K. Lee, M. K. Majumdar, D. Buyaner, J. K. Hendricks, M. F. Pittenger, J. D. Mosca, *Mol. Ther.* **2001**, *3*, 857.
[67] L. He, Y. Duan, J. Feng, Z. Wan, X. Liu, Y. Wang, F. Yu, Y. Wang, Y. Xiong, Y. Wu, *Sens. Actuators, B Chem.* **2020**, *323*, 128661.
[68] J. H. Wang, Y. M. Liu, J. Bin Chao, H. Wang, Y. Wang, S. M. Shuang, *Sens. Actuators, B Chem.* **2020**, *303*, 127216.
[69] R. Long, C. Tang, T. Li, X. Tong, C. Tong, Y. Guo, Q. Gao, L. Wu, S. Shi, *Microchim. Acta* **2020**, *187*, 307.
[70] S. Liu, Z. Liu, Q. Li, H. Xia, W. Yang, R. Wang, Y. Li, H. Zhao, B. Tian, *Spectrochim. Acta - Part A Mol. Biomol. Spectrosc.* **2021**, *246*, 118964.
[71] Z. Guo, Y. Jiao, F. Du, Y. Gao, W. Lu, S. Shuang, C. Dong, Y. Wang, *Talanta* **2020**, *216*, 120943.
[72] Garima, S. Jindal, S. Garg, I. Matai, G. Packirisamy, A. Sachdev, *Microchim. Acta* **2021**, *188*, 13.
[73] H. Zhang, Y. Gao, Y. Jiao, W. Lu, S. Shuang, C. Dong, *Analyst* **2020**, *145*, 2212.
[74] M. Abdesselem, R. Ramodiharilafy, L. Devys, T. Gacoin, A. Alexandrou, C. I. Bouzigues, *Nanoscale* **2017**, *9*, 656.
[75] L. Tan, Z. Chen, Y. Zhao, X. Wei, Y. Li, C. Zhang, X. Wei, X. Hu, *Biosens. Bioelectron.* **2016**, *85*, 414.
[76] S. Hamd-Ghadareh, A. Salimi, *Ionics* **2019**, *25*, 4469.
[77] C. Ding, S. Cheng, C. Zhang, Y. Xiong, M. Ye, Y. Xian, *Anal. Chem.* **2019**, *91*, 7181.
[78] Y. Zhang, D. Hou, X. Yu, *Spectrochim. Acta - Part A Mol. Biomol. Spectrosc.* **2020**, *234*, 118276.
[79] J. Liu, L. Pan, C. Shang, B. Lu, R. Wu, Y. Feng, W. Chen, R. Zhang, J. Bu, Z. Xiong, W. Bu, J. Du, J. Shi, *Sci. Adv.* **2020**, *6*, eaax9757.
[80] A. Nakamura, S. Tsukiji, *Bioorg. Med. Chem. Lett.* **2017**, *27*, 3127.
[81] S. Xu, X. He, Y. Huang, X. Liu, L. Zhao, X. Wang, Y. Sun, P. Ma, D. Song, *Microchim. Acta* **2020**, *187*, 478.
[82] C. Wang, Y. Wang, G. Wang, C. Huang, N. Jia, *Anal. Chim. Acta* **2020**, *1097*, 230.
[83] S. Xu, Y. Yu, Y. Gao, Y. Zhang, X. Li, J. Zhang, Y. Wang, B. Chen, *Microchim. Acta* **2018**, *185*, 454.
[84] X. Zhang, W. Zhang, Q. Wang, J. Wang, G. Ren, X. Dong Wang, *Microchim. Acta* **2019**, *186*, 584.
[85] X. X. Chen, L. Y. Niu, N. Shao, Q. Z. Yang, *Anal. Chem.* **2019**, *91*, 4301.
[86] S. Ludwanowski, A. Samanta, S. Loescher, C. Barner-Kowollik, A. Walther, *Adv. Sci.* **2021**, *8*, 2003740.
[87] C. Zhu, J. Yang, J. Zheng, S. Chen, F. Huang, R. Yang, *Anal. Chem.* **2019**, *91*, 15599.
[88] W. Cheng, X. Xue, L. Gan, P. Jin, B. Zhang, M. Guo, J. Si, H. Du, H. Chen, J. Fang, *Anal. Chim. Acta* **2021**, *1156*, 338362.
[89] Z. Zhang, J. Fan, J. Du, X. Peng, *Coord. Chem. Rev.* **2021**, *427*, 213575.
[90] J. Bai, X. Yang, Y. Qian, *J. Lumin.* **2020**, *221*, 117055.
[91] K. Yang, S. Wang, Y. Wang, H. Miao, X. Yang, *Biosens. Bioelectron.* **2017**, *91*, 566.
[92] Z. Fang, Z. Su, W. Qin, H. Li, B. Fang, W. Du, Q. Wu, B. Peng, P. Li, H. Yu, L. Li, W. Huang, *Chin. Chem. Lett.* **2020**, *31*, 2903.
[93] S. Tsuboi, T. Jin, *Chembiochem* **2019**, *20*, 568.
[94] F. Yang, F. Lin, J. Zhang, J. Qu, L. Wei, M. Du, T. Chen, Z. Mai, *Opt. Express* **2017**, *25*, 26089.
[95] Z. Ding, X. Dou, C. Wang, G. Feng, J. Xie, X. Zhang, *Nanotechnology* **2021**, *32*, 245502.
[96] S. Wang, L. Liu, Y. Fan, A. M. El-Toni, M. S. Alhoshan, D. Li, F. Zhang, *Nano Lett.* **2019**, *19*, 2418.
[97] B. Dong, S. Du, C. Wang, H. Fu, Q. Li, N. Xiao, J. Yang, X. Xue, W. Cai, D. Liu, *ACS Nano* **2019**, *13*, 1421.
[98] I. M. Khan, S. Niazi, M. K. Iqbal Khan, I. Pasha, A. Mohsin, J. Haider, M. W. Iqbal, A. Rehman, L. Yue, Z. Wang, *TrAC - Trends Anal. Chem.* **2019**, *119*, 115637.
[99] D. Wang, B. Z. Tang, *Acc. Chem. Res.* **2019**, *52*, 2559.
[100] F. Yan, X. Sun, T. Ma, Y. Zhang, Y. Jiang, R. Wang, C. Ma, J. Wei, L. Chen, Y. Cui, *Chem. Eng. J.* **2021**, *407*, 127801.
[101] L. Li, L. Shi, J. Jia, O. Eltayeb, W. Lu, Y. Tang, C. Dong, S. Shuang, *ACS Appl. Mater. Interfaces* **2020**, *12*, 18250.
[102] Q. Lu, J. Wang, B. Li, C. Weng, X. Li, W. Yang, X. Yan, J. Hong, W. Zhu, X. Zhou, *Anal. Chem.* **2020**, *92*, 7770.
[103] K. N. Wang, L. Y. Liu, D. Mao, S. Xu, C. P. Tan, Q. Cao, Z. W. Mao, B. Liu, *Angew. Chem. Int. Ed.* **2021**, *60*, 15095.
[104] B. Hellenkamp, S. Schmid, O. Doroshenko, O. Opanasyuk, R. Kühnemuth, S. Rezaei Adariani, B. Ambrose, M. Aznauryan, A. Barth, V. Birkedal, M. E. Bowen, H. Chen, T. Cordes, T. Eilert, C. Fijen, C. Gebhardt, M. Götz, G. Gouridis, E. Gratton, T. Ha, P. Hao, C. A. Hanke, A. Hartmann, J. Hendrix, L. L. Hildebrandt, V. Hirschfeld, J. Hohlbein, B. Hua, et al., *Nat. Methods* **2018**, *15*, 669.
[105] G. Bharathi, F. Lin, L. Liu, T. Y. Ohulchanskyy, R. Hu, J. Qu, *Colloids Surf. B Biointerfaces* **2021**, *198*, 111458.
[106] J. Roszik, D. Lisboa, J. Szöllősi, G. Vereb, *Cytom. Part A* **2009**, *75A*, 761.
[107] S. Lee, D. A. Abed, L. J. Beamer, L. Hu, *SLAS Discovery* **2021**, *26*, 100.
[108] F. Yang, C. Wang, L. Wang, Z. W. Ye, X. B. Song, Y. Xiao, *Chin. Chem. Lett.* **2017**, *28*, 2019.
[109] L. Rong, S. Y. Qin, C. Zhang, Y. J. Cheng, J. Feng, S. B. Wang, X. Z. Zhang, *Mater. Today Chem.* **2018**, *9*, 91.
[110] Y. Geng, H. L. Goel, N. B. Le, T. Yoshii, R. Mout, G. Y. Tonga, J. J. Amante, A. M. Mercurio, V. M. Rotello, *Nanomed. Nanotechnol. Biol. Med.* **2018**, *14*, 1931.
[111] Y. Zhang, S. He, W. Chen, Y. Liu, X. Zhang, Q. Miao, K. Pu, *Angew. Chem. Int. Ed.* **2021**, *60*, 5921.
[112] H. J. Cho, S. Lee, S. J. Park, Y. D. Lee, K. Jeong, J. H. Park, Y. S. Lee, B. Kim, H. S. Jeong, S. Kim, *Colloids Surf. B Biointerfaces* **2019**, *179*, 9.
[113] E. Campbell, M. T. Hasan, R. Gonzalez Rodriguez, G. R. Akkaraju, A. V. Naumov, *ACS Biomater. Sci. Eng.* **2019**, *5*, 4671.
[114] Y. C. Chan, M. H. Chan, C. W. Chen, R. S. Liu, M. Hsiao, D. P. Tsai, *ACS Omega* **2018**, *3*, 1627.
[115] N. Kim, E. Kim, H. Kim, M. R. Thomas, A. Najer, M. M. Stevens, *Adv. Mater.* **2021**, *33*, 2007738.
[116] T. Hianik, In *Encyclopedia Of Interfacial Chemistry: Surface Science And Electrochemistry*, Elsevier, Amsterdam, Netherlands **2018**, pp. 11–19.

[117] X. Zheng, R. Peng, X. Jiang, Y. Wang, S. Xu, G. Ke, T. Fu, Q. Liu, S. Huan, X. Zhang, *Anal. Chem.* **2017**, *89*, 10941.
[118] Y. Du, P. Peng, T. Li, *ACS Nano* **2019**, *13*, 5778.
[119] J. Han, K. Burgess, *Chem. Rev.* **2010**, *110*, 2709.
[120] S. Ghosh, Y. F. Chang, D. M. Yang, S. Chattopadhyay, *Biosens. Bioelectron.* **2020**, *155*, 112115.
[121] A. Kaur, K. Sapkota, S. Dhakal, *ACS Sens.* **2019**, *4*, 623.
[122] W. Chen, J. Han, J. She, F. Wang, L. Zhu, R. Q. Yu, J. H. Jiang, *Chem. Commun.* **2020**, *56*, 7797.
[123] S. Ye, H. Zhang, J. Fei, C. H. Wolstenholme, X. Zhang, *Angew. Chem. Int. Ed.* **2021**, *60*, 1339.
[124] S. Finkbeiner, *Cold Spring Harbor Perspect. Biol.* **2011**, *3*, a007476.
[125] N. H. Mudliar, P. M. Dongre, P. K. Singh, *Int. J. Biol. Macromol.* **2021**, *167*, 1371.
[126] P. Rodríguez-Sevilla, F. Sanz-Rodríguez, R. P. Peláez, R. Delgado-Buscalioni, L. Liang, X. Liu, D. Jaque, *Adv. Biosyst.* **2019**, *3*, 1900082.
[127] S. Tarapcsák, G. Szalóki, Á. Telbisz, Z. Gyöngy, K. Matúz, É. Csosz, P. Nagy, I. J. Holb, R. Rühl, L. Nagy, G. Szabó, K. Goda, *Sci. Rep.* **2017**, *7*, 41376.
[128] I. E. Steinmark, P. H. Chung, R. M. Ziolek, B. Cornell, P. Smith, J. A. Levitt, C. Tregidgo, C. Molteni, G. Yahioglu, C. D. Lorenz, K. Suhling, *Small* **2020**, *16*, 1907139.
[129] H. Soleimaninejad, M. Z. Chen, X. Lou, T. A. Smith, Y. Hong, *Chem. Commun.* **2017**, *53*, 2874.
[130] J. S. Donner, S. A. Thompson, M. P. Kreuzer, G. Baffou, R. Quidant, *Nano Lett.* **2012**, *12*, 2107.
[131] J. S. Donner, S. A. Thompson, C. Alonso-Ortega, J. Morales, L. G. Rico, S. I. C. O. Santos, R. Quidant, *ACS Nano* **2013**, *7*, 8666.
[132] G. Spicer, A. Efeyan, A. P. Adam, S. A. Thompson, *J. Biophotonics* **2019**, *12*, 201900044.
[133] S. A. Thompson, I. A. Martínez, P. Haro-González, A. P. Adam, D. Jaque, J. B. Nieder, R. De La Rica, *ACS Photonics* **2018**, *5*, 2676.
[134] G. Spicer, S. Gutierrez-Erlandsson, R. Matesanz, H. Bernard, A. P. Adam, A. Efeyan, S. Thompson, *J. Biophotonics* **2021**, *14*, 202000341.
[135] A. Nexha, J. J. Carvajal, M. C. Pujol, F. Díaz, M. Aguiló, *Nanoscale* **2021**, *13*, 7913.
[136] J. Zhou, B. del Rosal, D. Jaque, S. Uchiyama, D. Jin, *Nat. Methods* **2020**, *17*, 967.
[137] A. Bednarkiewicz, J. Drabik, K. Trejgis, D. Jaque, E. Ximendes, L. Marciniak, *Appl. Phys. Rev.* **2021**, *8*, 011317.
[138] X. Di, D. Wang, J. Zhou, L. Zhang, M. H. Stenzel, Q. P. Su, D. Jin, *Nano Lett.* **2021**, *21*, 1651.
[139] F. Shang, C. Hu, W. Xu, X. Zhu, D. Zhao, W. Zhang, Z. Zhang, W. Cao, *J. Alloys Compd.* **2021**, *858*, 157637.
[140] Z. Sun, M. Jia, Z. Fu, M. Zhang, H. Wang, Y. Xu, *Chem. Eng. J.* **2021**, *406*, 126755.
[141] M. Nakano, Y. Arai, I. Kotera, K. Okabe, Y. Kamei, T. Nagai, *PLoS One* **2017**, *12*, e0172344.
[142] I. E. Kolesnikov, M. A. Kurochkin, I. N. Meshkov, R. A. Akasov, A. A. Kalinichev, E. Y. Kolesnikov, Y. G. Gorbunova, E. Lähderanta, *Mater. Des.* **2021**, *203*, 109613.
[143] Z. Huang, N. Li, X. Zhang, Y. Xiao, *Anal. Chem.* **2021**, *93*, 5081.
[144] J. Qiao, C. Chen, D. Shangguan, X. Mu, S. Wang, L. Jiang, L. Qi, *Anal. Chem.* **2018**, *90*, 12553.
[145] J. Liu, H. Zhang, G. S. Selopal, S. Sun, H. Zhao, F. Rosei, *ACS Photonics* **2019**, *6*, 2479.
[146] Y. Han, Y. Liu, H. Zhao, A. Vomiero, R. Li, *J. Mater. Chem. B* **2021**, *9*, 4111.
[147] A. Carattino, M. Caldarola, M. Orrit, *Nano Lett.* **2018**, *18*, 874.
[148] O. A. Savchuk, O. F. Silvestre, R. M. R. Adão, J. B. Nieder, *Sci. Rep.* **2019**, *9*, 1.
[149] S. Elumalai, S. Managó, A. C. De Luca, *Sensors* **2020**, *20*, 5525.
[150] D. Zhang, D. Jiang, M. Yanney, S. Zou, A. Sygula, *Anal. Biochem.* **2009**, *391*, 121.
[151] L. E. Jamieson, A. Li, K. Faulds, D. Graham, *R. Soc. Open Sci.* **2018**, *5*, 181483.
[152] G. M. Knudsen, B. M. Davis, S. K. Deb, Y. Loethen, R. Gudihal, P. Perera, D. Ben-Amotz, V. J. Davisson, *Bioconjugate Chem.* **2008**, *19*, 2212.
[153] Y. Su, D. Wu, J. Chen, G. Chen, N. Hu, H. Wang, P. Wang, H. Han, G. Li, Y. Wu, *Anal. Chem.* **2019**, *91*, 11687.
[154] L. E. Jamieson, C. Wetherill, K. Faulds, D. Graham, *Chem. Sci.* **2018**, *9*, 6935.
[155] I. J. Jahn, A. Mühlig, D. Cialla-May, *Anal. Bioanal. Chem.* **2020**, *412*, 5999.
[156] L. T. Wilson, W. J. Tipping, C. Wetherill, Z. Henley, K. Faulds, D. Graham, S. P. Mackay, N. C. O. Tomkinson, *Anal. Chem.* **2021**, *93*, 12786.
[157] A. Pallaoro, G. B. Braun, M. Moskovits, *Proc. Natl. Acad. Sci.* **2011**, *108*, 16559.
[158] E. Garai, S. Sensarn, C. L. Zavaleta, D. Van de Sompel, N. O. Loewke, M. J. Mandella, S. S. Gambhir, C. H. Contag, *J. Biomed. Opt.* **2013**, *18*, 1.
[159] J. Noonan, S. M. Asiala, G. Grassia, N. MacRitchie, K. Gracie, J. Carson, M. Moores, M. Girolami, A. C. Bradshaw, T. J. Guzik, G. R. Meehan, H. E. Scales, J. M. Brewer, I. B. McInnes, N. Sattar, K. Faulds, P. Garside, D. Graham, P. Maffia, *Theranostics* **2018**, *8*, 6195.
[160] A. K. Ilkhechi, C. N. Bergman, F. R. Wuest, J. Dufour, J. D. Lewis, K. L. Bell, P. Kedarisetti, R. J. Paproski, R. J. Zemp, V. R. Bouvet, W. Shi, *Biomed. Opt. Express* **2020**, *11*, 6211.
[161] J. Du, Y. Su, C. Qian, D. Yuan, K. Miao, D. Lee, A. H. C. Ng, R. S. Wijker, A. Ribas, R. D. Levine, J. R. Heath, L. Wei, *Nat. Commun.* **2020**, *11*, 1.
[162] L. Peng, in *Methods in Molecular Biology*, Humana, New York, NY, **2021**, pp. 157–172.
[163] M. Tan, B. del Rosal, Y. Zhang, E. M. Rodríguez, J. Hu, Z. Zhou, R. Fan, D. H. Ortgies, N. Fernández, I. Chaves-Coira, Á. Núñez, D. Jaque, G. Chen, *Nanoscale* **2018**, *10*, 17771.
[164] Y. Lu, J. Zhao, R. Zhang, Y. Liu, D. Liu, E. M. Goldys, X. Yang, P. Xi, A. Sunna, J. Lu, Y. Shi, R. C. Leif, Y. Huo, J. Shen, J. A. Piper, J. P. Robinson, D. Jin, *Nat. Photonics* **2013**, *8*, 32.
[165] K. T. Haas, M. W. Fries, A. R. Venkitaraman, A. Esposito, *Front. Phys.* **2021**, *9*, 291.
[166] M. Bates, G. T. Dempsey, K. H. Chen, X. Zhuang, *ChemPhysChem* **2012**, *13*, 99.
[167] M. Bates, B. Huang, G. T. Dempsey, X. Zhuang, *Science* **2007**, *317*, 1749.
[168] B. Huang, S. A. Jones, B. Brandenburg, X. Zhuang, *Nat. Methods* **2008**, *5*, 1047.
[169] M. S. Gunewardene, F. V. Subach, T. J. Gould, G. P. Penoncello, M. V. Gudheti, V. V. Verkhusha, S. T. Hess, *Biophys. J.* **2011**, *101*, 1522.
[170] H. Shroff, C. G. Galbraith, J. A. Galbraith, H. White, J. Gillette, S. Olenych, M. W. Davidson, E. Betzig, *Proc. Natl. Acad. Sci.* **2007**, *104*, 20308.
[171] I. Testa, C. A. Wurm, R. Medda, E. Rothermel, C. Von Middendorf, J. Fölling, S. Jakobs, A. Schönle, S. W. Hell, C. Eggeling, *Biophys. J.* **2010**, *99*, 2686.
[172] D. Baddeley, D. Crossman, S. Rossberger, J. E. Cheyne, J. M. Montgomery, I. D. Jayasinghe, C. Cremer, M. B. Cannell, C. Soeller, *PLoS One* **2011**, *6*, e20645.
[173] G. Donnert, J. Keller, C. A. Wurm, S. O. Rizzoli, V. Westphal, A. Schönle, R. Jahn, S. Jakobs, C. Eggeling, S. W. Hell, *Biophys. J.* **2007**, *92*, L67.

[174] M. Kamper, H. Ta, N. A. Jensen, S. W. Hell, S. Jakobs, *Nat. Commun.* **2018**, *9*, 4762.
[175] D. S. Richardson, C. Gregor, F. R. Winter, N. T. Urban, S. J. Sahl, K. I. Willig, S. W. Hell, *Nat. Commun.* **2017**, *8*, 1.
[176] A. G. Tebo, B. Moeyaert, M. Thauvin, I. Carlon-Andres, D. Böken, M. Volovitch, S. Padilla-Parra, P. Dedecker, S. Vriz, A. Gautier, *Nat. Chem. Biol.* **2021**, *17*, 30.
[177] A. Dani, B. Huang, J. Bergan, C. Dulac, X. Zhuang, *Neuron* **2010**, *68*, 843.

Paloma Rodríguez-Sevilla completed her Ph.D. on optical manipulation of upconverting particles for biological studies in 2017 at the Universidad Autónoma de Madrid (Spain). She then joined the Optical Manipulation group as a research fellow at the University of St Andrews (UK). Currently, she is working in the development of new photonic sensing techniques as a Juan de la Cierva Incorporación fellow in the Nanomaterials for Bioimaging Group at the Universidad Autónoma de Madrid.

Sebastian A. Thompson is currently leading his own group at IMDEA Nanosciences in Madrid (Spain) (thompson-lab.net). His lab is focused on intracellular temperature measurements for cancer research and diagnostics. He received his Ph.D. at Hunter College, City University of New York (USA). After his postdoctoral stances at the Institute of Photonics Science (Spain), Northwestern University (USA), and the National Center of Oncology Research (Spain), he received the prestigious European fellowship Marie Skłodowska-Curie at the University of Coimbra (Portugal). He combines his research with teaching activities at the City University of New York and the Complutense University of Madrid (Spain).

Daniel Jaque got his Ph.D. in physics from Universidad Autónoma de Madrid (Spain) in 1999. After a decade of outstanding research on laser materials and photonics, he founded the Fluorescence Imaging Group together with Prof. J. García Solé in 2010, which has been working to develop luminescent materials nanomaterials of different kinds (quantum dots, lanthanide-doped nanoparticles, etc.) toward applications ranging from optical trapping to biomedical imaging. Prof. Jaque was a pioneer from the dawn of luminescence thermometry; today, he is a world-renowned leader in the in vivo application of this technique.